Thirty minutes later, the animals were injected intraperitoneally with saline or milnacipran (30 mg/kg) or CP94253 (5 mg/kg), a selective 5-HT1B receptor agonist or mCPP (5 mg/kg), a 5-HT2C/1B receptor agonist. Thirty minutes later, they were given chow pellets, and pellet intake was measured for the next 1 h.

In *experiment 4*, 5-wk-old male A^y mice and wild-type littermates were deprived of food for 23 h. The following morning, the animals were intraperitoneally injected with saline or milnacipran (30 mg/kg) 30 min before food presentation. Intake of chow pellets was measured for the next 1 h.

In *experiment 5*, 5-wk-old male A^y mice and wild-type littermates were intraperitoneally injected with saline or milnacipran (30 mg/kg) 30 min before the onset of the dark cycle. Intake of chow pellets was measured for the next hour after onset of the dark cycle.

In *experiment 6*, 8-wk-old male A^y mice and wild-type littermates were intraperitoneally injected with saline or milnacipran (30 mg/kg) twice daily (at 1000 and 1800) for 3 days. Daily food intake and body weight were measured.

In *experiment 7*, 5-wk-old male A^y mice and wild-type littermates, which were provided 3.5 g of chow pellets daily for 5 days before the experiment, were intraperitoneally injected with saline or milnacipran (30 mg/kg) or fenfluramine (3 mg/kg). Chow pellets were provided 30 min later. Intake of chow pellets was measured for the next hour. The experiment was performed between 1000 and 1200.

In *experiment 8*, 5-wk-old C57BL6J mice were intraperitoneally injected with saline or milnacipran (30 mg/kg) in the light and dark cycle. In the dark cycle, drugs were administered between 2000 and 2030. Animals were not fed chow pellets. After 30, 60, or 120 min, the separate groups of animals were decapitated, and blood was collected for measurement of glucose and corticosterone levels in the light cycle. In a separate group of animals, 60 and 120 min later, the hypothalamus was removed for RNA extraction in the light cycle. Moreover, after 60 or 120 min, the separate groups of animals were decapitated and blood was collected for measurement of corticosterone levels in the dark cycle. Whole blood was mixed with EDTA-2Na (2 mg/ml) to determine plasma corticosterone levels.

Finally, 5-wk-old C57BL6J mice were intraperitoneally injected with saline or fenfluramine (3 mg/kg). They were not fed chow pellets. Sixty minutes later, the animals were decapitated, and the hypothalamus was removed for RNA extraction. Blood was collected for the measurement of glucose and corticosterone levels. Whole blood was mixed with EDTA-2Na (2 mg/ml) to determine plasma corticosterone levels.

The dose of fenfluramine (3 mg/kg) was based on the evidence that fenfluramine-induced hypophagia is attenuated by a genetic blockade of 5-HT2C receptors (28). The dose of SB242084 (2 mg/kg) eliminates 5-HT2C receptor functions in vivo as described previously (13, 22). The dose of SB224289 dihydrochloride (5 mg/kg) eliminates 5-HT1B receptor functions in vivo (15, 16, 22).

The animal studies were conducted under protocols in accordance with the institutional guidelines for animal experiments at Tohoku University Graduate School of Medicine.

Real-time quantitative RT-PCR. Total RNA was isolated from mouse hypothalamic tissue using the RNeasy Midi kit (Qiagen, Hilden, Germany), according to the manufacturer's directions, and cDNA synthesis was performed using a Super Script III First-Strand Synthesis System for RT-PCR Kit (Invitrogen, Rockville, MD) using 1 μg total RNA. cDNA synthesized from total RNA was evaluated in a real-time PCR quantitative system (Light Cycler Quick System 350S; Roche Diagnostics, Mannheim, Germany). The primers used were as follows. For mouse proopiomelanocortin (POMC), sense, 5′-ATA GAT GTG TGG AGC TGG TG-3′, antisense, 5′-GGC TGT TCA TCT CCG TTG-3′; for mouse cocaine- and amphetamine-regulated transcript (CART), sense, 5′-CTG GACATC TAC TCT GCC GTG G-3′, antisense, 5′-GTT CCT CGG GGA CAG TCA CAC AGC-3′; for mouse neuropeptide Y (NPY), sense, 5′-GCT TGA AGA CCC TTC CAT TGG TG-3′, antisense, 5′-GGC GGA GTC CAG CCT AGT GG-3′; for mouse ghrelin, sense, 5′-GAA AGG AAT CCA AGA AGC CA-3′, antisense, 5′-GCT TGA TGC CAA CAT CGA A-3′; for mouse corticotropin releasing hormone (CRH), sense, 5′-CCG GGC AGA GCA GTT AGC-3′, antisense, 5′-CAA CAT TTC ATT TCC CGA TAA TCT C-3′, for mouse suppressor of cytokine signaling-3 (SOCS-3), sense, 5′-GCG GGC ACC TTT CTT ATC C-3′, antisense, 5′-TCC CCG ACT GGG TCT TGA C-3′, and for mouse β-actin, sense, 5′-TTG TAA CCA ACT GGG ACG ATA TGG-3′, antisense, 5′-GAT CTT GAT CTT CAT GGT GCT AGG-3′. The relative amount of mRNA was calculated with β-actin mRNA as the invariant control. The data are shown as the fold change of the mean value of the control group, which received saline.

Blood chemistries. Blood glucose levels were measured by glucose strips (Freestyle blood glucose monitoring system; Kasei, Tokyo, Japan). Plasma active ghrelin levels were measured by ELISA (Active ghrelin ELISA kit, Mitsubishi Kagaku Iatron, Tokyo, Japan). Plasma corticosterone levels were measured by radioimmunoassay (Linco, St. Louis, MO).

Statistical methods. Data are presented as the means ± SE. Statistical significance of differences between two groups was determined using Student's *t*-test. Comparisons among more than two groups were done by analysis of variance using Bonferroni's correction for multiple comparisons. A P value of less than 0.05 was considered statistically significant.

RESULTS

Dose-response effects and time course of the effects of milnacipran on food intake. To determine the dose-response effects of milnacipran on food intake, we examined food intake after the administration of milnacipran (3–60 mg/kg) or saline in C57BL6J mice. Administration of milnacipran (20–60 mg/kg) significantly reduced food intake in C57BL6J mice (to ~67%–70% that of saline controls). Lower doses of milnacipran (3–10 mg/kg) had no effect on food intake during a 1-h feeding period after a 23-h fast in C57BL6J mice (Fig. 1*A*). To further determine the time course of the effects of milnacipran on food intake, we examined food intake after administration of milnacipran (30 mg/kg) or saline in C57BL6J mice. The doses of milnacipran to induce anorexic effects were within the range to induce antidepressive effects in rodents (18, 25). In addition, the anorexic effects of milnacipran (30 mg/kg) were sustained for 5 h (Fig. 1*B*).

To determine the effects of selective 5-HT2C and 5-HT1B receptor antagonists on the anorexic effects of milnacipran, we intraperitoneally injected SB242084 (2 mg/kg) or SB224289 (5 mg/kg) 30 min before administering the milnacipran (30 mg/kg). Neither SB242084 nor SB224289 reversed the feeding suppression induced by milnacipran (Fig. 1*C*). SB224289 (5 mg/kg) reversed the feeding suppression induced by CP94253 (5 mg/kg; Fig. 1*D*). SB242084 (2 mg/kg) partially but significantly reversed the feeding suppression induced by mCPP (5 mg/kg) (Fig. 1*E*). SB242084 and SB224289 alone had no effects on food intake as described previously (22).

Effects of milnacipran on food intake and body weight in A^y mice. To determine the effects of milnacipran on food intake on A^y mice, we administered milnacipran to nonobese (5-wk-old) A^y mice and wild-type mice. Milnacipran (30 mg/kg) significantly reduced food intake in wild-type mice and A^y mice (to ~68% and 48% that of controls,

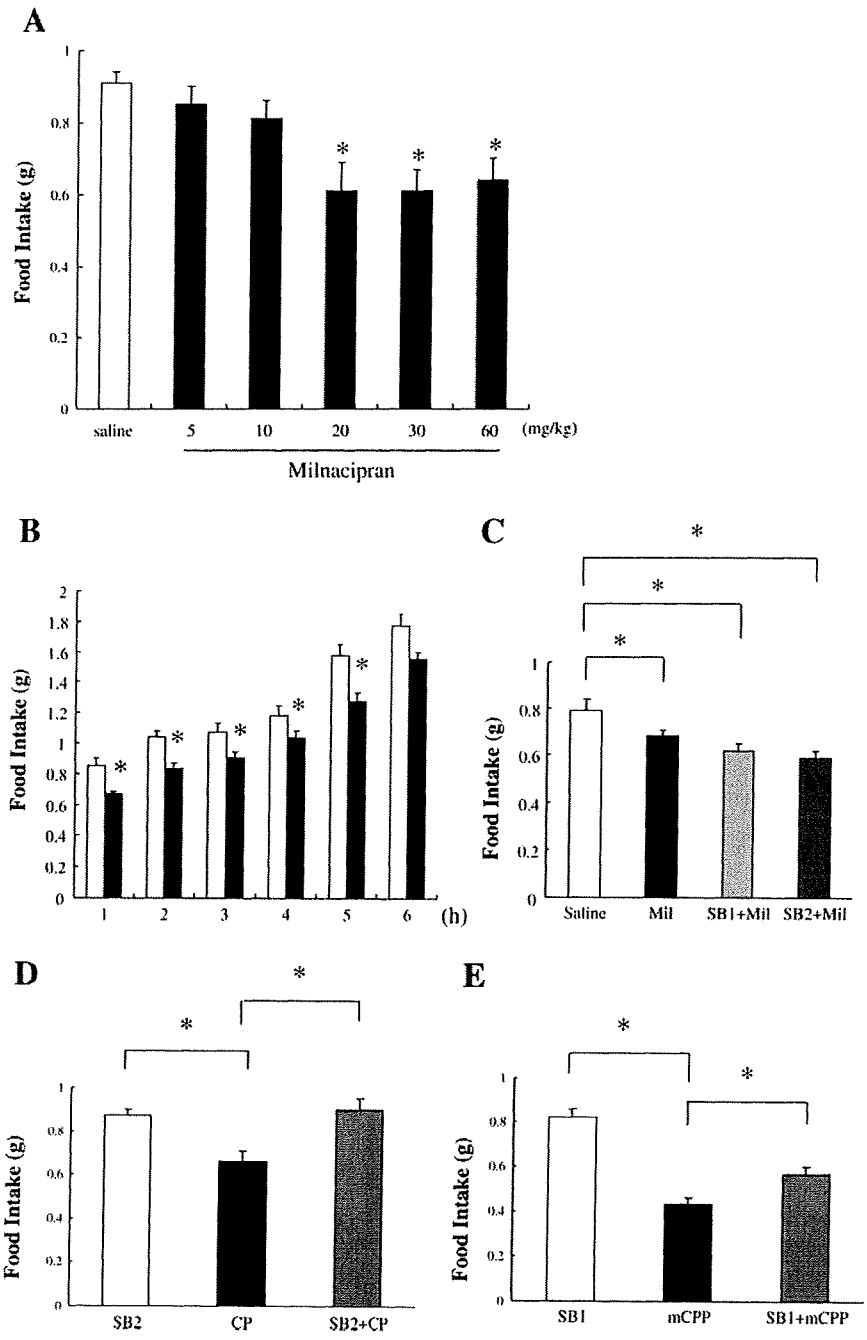

Fig. 1. Dose-response effects of milnacipran on food intake (*A*), time course of the effects of milnacipran (30 mg/kg) on food intake (*B*), and the effects of a selective 5-HT2C receptor antagonist, SB242084, and a selective 5-HT1B receptor antagonist, SB224289, on the feeding suppression induced by milnacipran (*C*), the effects of SB224289 on the feeding suppression induced by CP94253 (*D*), and the effects of SB242084 on the feeding suppression induced by m-chlorophenylpiperazine (mCPP; *E*) in C57BL6J mice. After a 23-h fast, mice were intraperitoneally injected with milnacipran, CP94253, mCPP, or saline. Open bar, saline; solid bars, milnacipran (3–60 mg/kg). SB1, SB242084 (2 mg/kg); SB2, SB224289 (5 mg/kg); CP, CP94253 (5 mg/kg); mCPP (5 mg/kg). Values are expressed as the means ± SE of 7 or 8 animals. $^*P < 0.05$ vs. saline.

respectively) during the first hour of the feeding period after a 23-h fast (Fig. 2*A*).

To further confirm these results, we determined the effects of milnacipran on food intake in A^y mice and wild-type mice for the first hour after onset of the dark cycle. Milnacipran significantly reduced food intake in wild-type mice (to ~70% and 44% that of controls, respectively) during the first hour after onset of the dark cycle (Fig. 2*B*). These results suggest that milnacipran suppresses food intake in A^y mice.

Moreover, we determined the chronic effects of milnacipran on food intake and body weight in obese (8-wk-old) A^y mice and wild-type mice. Mice received milnacipran (30 mg/kg) or saline twice daily for three consecutive days. A^y mice had elevated baseline food intake and body weight relative to levels in wild-type mice (food intake: WT 3.5 ± 0.2 g, A^y 5.1 ± 0.1 g; $P < 0.05$; body weight: WT 29.4 ± 0.5 g, A^y 37.5 ± 0.5 g; $P < 0.05$, $n = 14–18$). Milnacipran administration reduced food intake and body weight in both A^y mice and wild-type mice (Fig. 3, *A–D*).

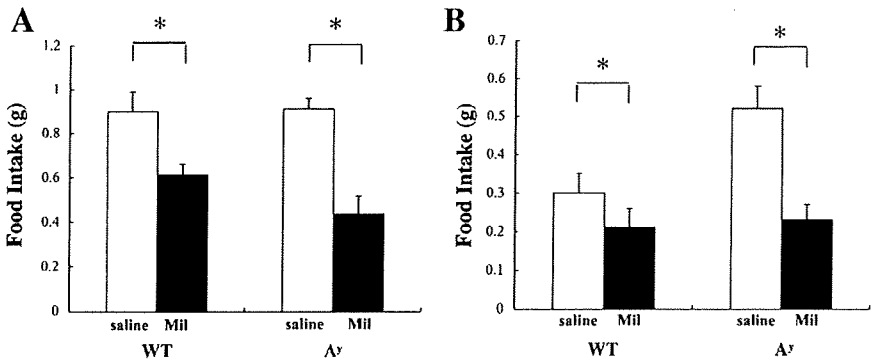

Fig. 2. Effects of milnacipran on food intake in 5-wk-old male A^y mice and wild-type mice. Mice were intraperitoneally injected with milnacipran or saline. Effects of milnacipran (30 mg/kg) on food intake in wild-type mice and A^y mice after a 23-h fast (*A*) and after onset of the dark cycle (*B*). Each column and bar represent the mean ± SE of 7 or 8 mice. Basal body weight: WT saline controls (open bars), 18.8 ± 0.7 g (*A*) and 24.0 ± 0.1 g (*B*); WT milnacipran treatment group (solid bars), 18.7 ± 0.7 g (*A*) and 23.8 ± 0.2 g (*B*); A^y saline controls (open bars), 21.4 ± 0.5 g (*A*) and 24.0 ± 0.3 g (*B*); A^y milnacipran treatment group (solid bars), 21.4 ± 0.3 g (*A*) and 24.1 ± 0.2 g (*B*). WT, wild-type; Mil, milnacipran. *$P < 0.05$.

Effects of restricted feeding on the responsiveness to milnacipran or fenfluramine in 5-wk-old A^y mice. We previously reported that restricted feeding (3.5 g/days for 5 days) decreased hypothalamic 5-HT2C and 5-HT1B receptor gene expression and attenuated the responsiveness of mCPP, a 5-HT2C/1B receptor agonist in food-restricted A^y mice compared with wild-type mice (23). To determine whether 5-HT2C and 5-HT1B receptors contribute to the appetite-suppressing effects of milnacipran, we examined the effects of restricted feeding (3.5 g/days for 5 days) on the responsiveness to milnacipran or fenfluramine in 5-wk-old A^y mice and wild-type mice. Both A^y mice and wild-type mice consumed 3.5 g of food during the light cycle for 5 days and were fasted during the dark cycle. After a 15-h fast, fenfluramine (3 mg/kg) had no effect on food intake in food-restricted A^y mice, whereas it significantly suppressed food intake in food-restricted wild-type mice (Fig. 4*A*). In contrast, milnacipran had no effects on food-restricted A^y mice and wild-type mice (Fig. 4*B*).

Effects of milnacipran on the expression of hypothalamic genes involved in the regulation of feeding and energy homeostasis. To determine the central mechanisms of the anorexic effects induced by milnacipran, we examined the expression of hypothalamic orexigenic peptides and anorexigenic peptides, which have important roles in the regulation of feeding (10). Milnacipran significantly increased hypothalamic POMC and CART mRNA levels compared with saline controls (1.6-fold and 1.3-fold compared with saline controls, respectively) at 1 h and had no significant effects on hypothalamic ghrelin, NPY, CRH, and SOCS-3 mRNA levels (Fig. 5). Milnacipran had no significant effects on hypothalamic POMC, CART, ghrelin, NPY, CRH, and SOCS-3 mRNA levels at 2 h (data not shown).

Effects of milnacipran and fenfluramine on plasma corticosterone and blood glucose levels. Milnacipran (30 mg/kg) had no effect on blood glucose and plasma corticosterone levels at 30 and 60 min after administration, while at 120 min, it significantly reduced both compared with saline controls in the light cycle (Fig. 6, *A* and *B*). In the dark cycle, milnacipran significantly reduced plasma corticosterone levels at 60 min and 120 min (Fig. 6*C*). Fenfluramine (3 mg/kg) significantly increased plasma corticosterone and blood glucose levels and increased hypothalamic CRH mRNA levels compared with saline controls at 1 h (Fig. 7, *A–C*).

DISCUSSION

The previous and present studies demonstrate that fenfluramine and milnacipran induce appetite-suppressing effects and increase hypothalamic POMC and CART gene expression in mice (21). The effects of these drugs on plasma corticosterone and blood glucose levels, however, differed. Activation of brain 5-HT systems increases plasma corticosterone levels associated with activation of hypothalamic CRH neurons, which induce anorexic effects (4, 9, 14). The results of the present study demonstrate that milnacipran did not increase plasma corticosterone levels and hypothalamic CRH gene expression, whereas fenfluramine increased both of them. Because milnacipran had no effect on hypothalamic CRH gene expression, it is reasonable that milnacipran did not increase plasma corticosterone levels. It might also be due to the basic actions of milnacipran, which inhibits 5-HT and NE reuptake but does not directly stimulate 5-HT receptors and 5-HT release.

The present results also demonstrate that milnacipran does not increase blood glucose levels, whereas fenfluramine increases blood glucose levels. At least three different neural pathways, such as increased epinephrine, glucagon, and direct innervation of the liver, are involved in acute hyperglycemia mediated by the CNS (19, 20). Although the relative contribution of these pathways to acute hepatic glucose production can be altered by changes in central neurotransmission, epinephrine secreted from the adrenal medulla has an essential role in the CNS-mediated acute hyperglycemia in rodents (19, 20). Fenfluramine or mCPP-induced hyperglycemia is mediated by increased epinephrine secretion from the adrenal medulla (3, 4, 19, 20, 26). Milnacipran, however, does not seem to induce sympathetic nervous system-mediated acute hyperglycemia. Rather, milnacipran slightly reduced blood glucose levels at 120 min after administration.

The central MC pathway is suggested to mediate satiety signaling downstream of 5-HT2C receptors (12). A^y mice have dominant alleles at the agouti locus (*A*), which produces ectopic expression of the agouti peptide, an antagonist of the hypothalamic MC4 receptors and MC3 receptors (8, 17) and therefore display hyperphagia and obesity. A^y mice are reportedly resistant to the anorexic effects of fenfluramine (12) and consumed more food and gained more weight compared with age-matched wild-type mice. The results of the present study demonstrate that A^y mice are responsive to milnacipran-induced feeding suppression and that chronic treatment with

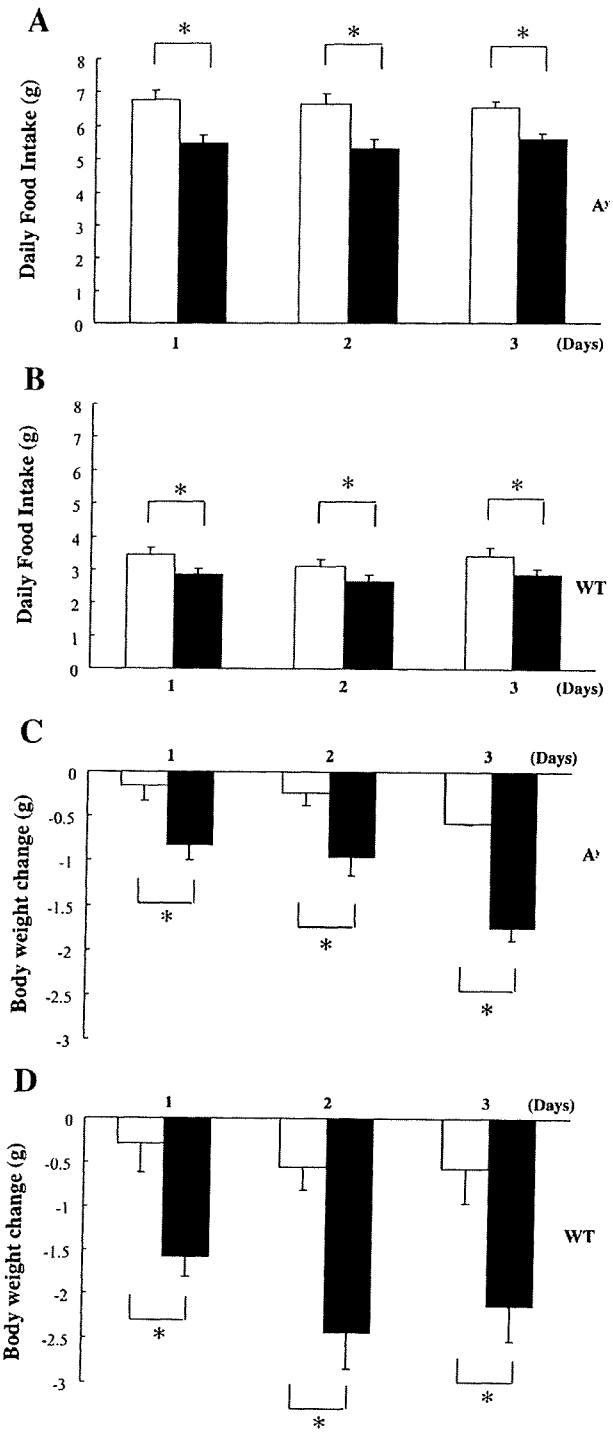

Fig. 3. Effects of chronic administered milnacipran on food intake (*A* and *B*) and body weight (*C* and *D*) in wild-type mice and obese (8-wk-old) A^y mice. Each column and bar represent the mean ± SE of 7–9 mice. Basal body weight: WT saline controls (open bars), 29.0 ± 0.7 g; WT milnacipran treatment group (solid bars), 29.8 ± 0.3 g; A^y saline controls (open bars), 37.7 ± 0.5 g; A^y milnacipran treatment group (solid bars), 37.6 ± 0.5 g. $*P < 0.05$.

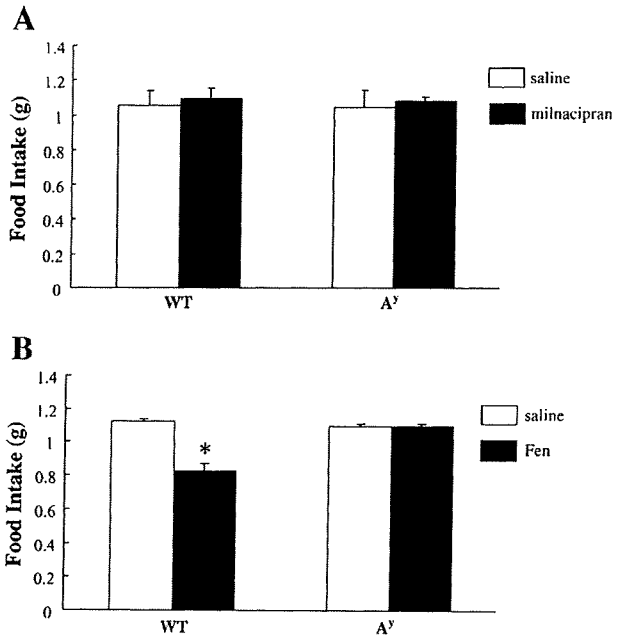

Fig. 4. Effects of restricted feeding on effects of milnacipran (*A*) and fenfluramine (*B*) on food intake in 5-wk-old A^y mice and WT mice. Mice were intraperitoneally injected with milnacipran (30 mg/kg) or fenfluramine (3 mg/kg) or saline. Basal body weight: WT saline controls (open bars), 20.2 ± 0.2 g; WT milnacipran (30 mg/kg) treatment group (solid bars), 21.3 ± 0.2 g; A^y saline controls (open bars), 21.8 ± 0.3 g; A^y fenfluramine (3 mg/kg) treatment group (solid bars), 22.4 ± 0.2 g. Data are presented as the mean values ± SE of 6 mice. $*P < 0.05$.

milnacipran suppresses hyperphagia and reduces body weight in obese A^y mice. These findings suggest that milnacipran induces appetite-suppressing effects through different neuronal mechanisms than fenfluramine.

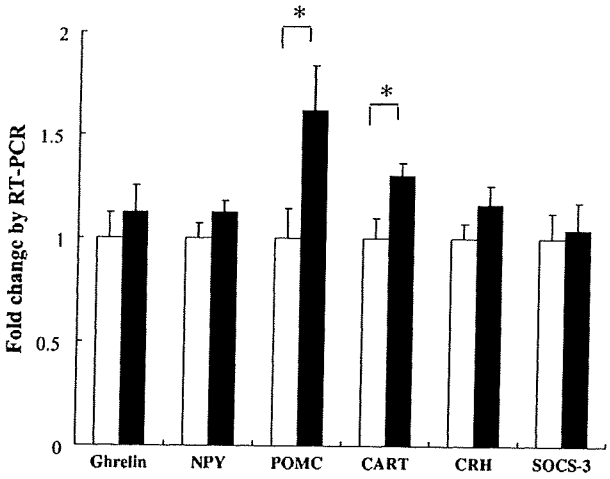

Fig. 5. Effects of milnacipran on hypothalamic ghrelin, neuropeptide Y (NPY), proopiomelanocortin (POMC), cocaine- and amphetamine-regulated transcript (CART), corticotropin-releasing hormone (CRH), and suppressor of cytokine signaling-3 (SOCS-3) mRNA levels in C57BL6J mice. Mice were intraperitoneally injected with milnacipran or saline. Open bar, saline; solid bars, milnacipran (30 mg/kg). Each column and bar represent the mean ± SE of 5 or 6 mice. $*P < 0.05$.

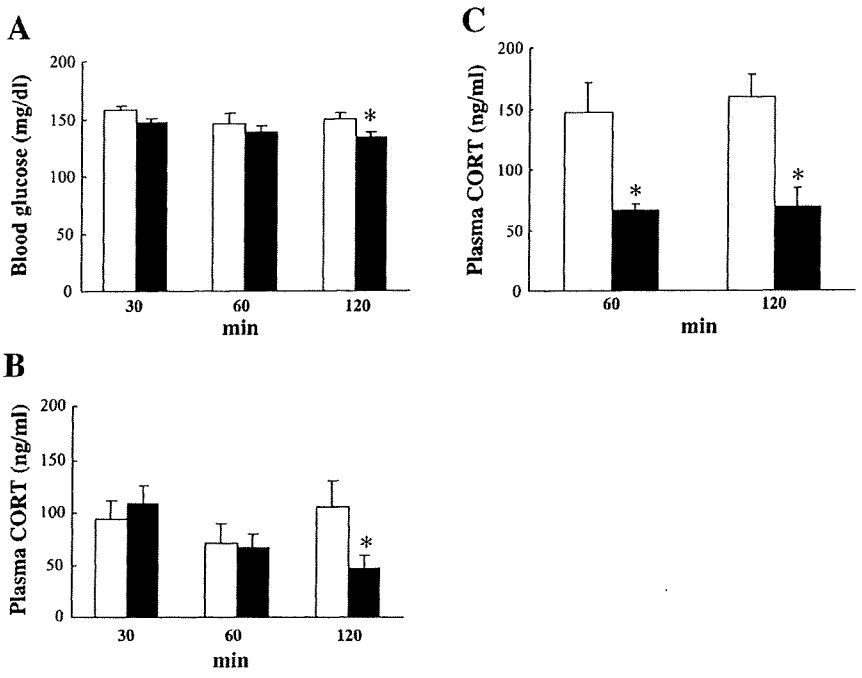

Fig. 6. Effects of milnacipran on and blood glucose levels (*A*) and plasma corticosterone (CORT) levels (*B*) in the light cycle, and plasma corticosterone levels (*C*) in the dark cycle of C57BL6J mice. Mice were intraperitoneally injected with milnacipran or saline. Blood glucose and plasma corticosterone levels were measured as described in the MATERIALS AND METHODS. Each column and bar represent the mean ± SE of 5 mice. Open bar, saline; solid bars, milnacipran (30 mg/kg). $*P < 0.05$.

Milnacipran interacts with POMC neurons in the hypothalamus and could stimulate POMC neurons to release enough alpha-melanocyte-stimulating hormone to overcome agouti blockade of MC receptors, because A^y mice are sensitive to MC agonist-induced feeding suppression (8). In addition, CART might contribute to the milnacipran-induced feeding suppression in A^y mice, possibly, because CART and MC neurons do not share a downstream pathway (2, 7). The present study demonstrates that 5-HT2C and 5-HT1B receptors are unlikely to mediate the appetite-suppressing effects of milnacipran. Inhibition of NE reuptake reportedly suppresses food intake and obesity in rats (11). Hypothalamic NE systems might therefore contribute to the appetite-suppressing effects and increased hypothalamic POMC and CART gene expres-

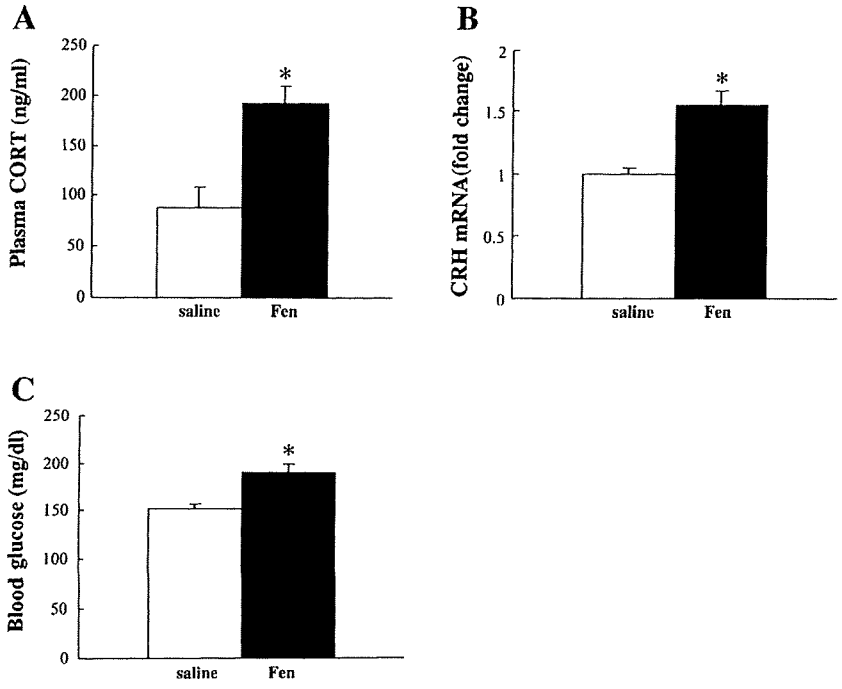

Fig. 7. Effects of fenfluramine (Fen) on plasma corticosterone levels (*A*), hypothalamic CRH mRNA levels (*B*), and blood glucose levels (*C*) in C57BL6J mice. Mice were intraperitoneally injected with milnacipran or saline. Blood glucose and plasma corticosterone levels were measured as described in the MATERIALS AND METHODS. Each column and bar represent the mean ± SE of 5 or 6 mice. Open bar, saline; solid bars, Fen (3 mg/kg). $*P < 0.05$.

sion of milnacipran without stimulating the HPA and sympathetic-adrenal medullary axis.

Other investigators previously reported that A^y mice are resistant to the anorexic effects of fenfluramine (12). Our previous and present studies, however, demonstrated that hyperphagic A^y mice are responsive to mCPP and fenfluramine-induced appetite suppression, whereas food-restricted A^y mice are resistant to them (23). We previously reported that hypothalamic 5-HT2C and 5-HT1B receptor gene expression was increased in nonobese hyperphagic A^y mice, whereas it was decreased by food restriction (23). Accordingly, the discrepancy between our results and previous results by other investigators might be due to the differences in feeding states of A^y mice.

In addition, our present study demonstrate that hyperphagic A^y mice are responsive to milnacipran-induced appetite suppression, whereas food restricted A^y mice are resistant to them (23). Moreover, food restricted wild-type mice are resistant to milnacipran-induced appetite suppression, whereas they are responsive to fenfluramine-induced appetite suppression.

These results support that 5-HT2C and 5-HT1B receptors are unlikely to contribute to the appetite-suppressing effects of milnacipran. The appetite-suppressing effects of milnacipran are also different than those of fluvoxamine, a selective 5-HT reuptake inhibitor, because fluvoxamine alone had no effects on feeding, and fluvoxamine and 5-HT2C receptor inactivation exert appetite-suppressing effects via 5-HT1B receptors (22).

In summary, these results suggest that inhibition of 5-HT and NA reuptake induces appetite-suppressing effects independent of 5-HT2C and 5-HT1B receptors and increases hypothalamic POMC and CART gene expression without stimulating the HPA axis or increasing blood glucose levels in mice. Restricted feeding can attenuate the milnacipran-induced appetite-suppressing effects.

ACKNOWLEDGMENTS

We thank Youko Hasegawa for the experimental assistance. This work was supported by a Grant-in-Aid for Scientific Research (C2) and Human Science Research (KH21016).

REFERENCES

1. **Boyer P, Briley M.** Milnacipran, a new specific serotonin and noradrenaline reuptake inhibitor. *Drugs Today* 34: 709–720, 1998.
2. **Broberger C.** Hypothalamic cocaine- and amphetamine-regulated transcript (CART) neurons: histochemical relationship to thyrotropin-releasing hormone, melanin concentrating hormone, orexin/hypocretin and neuropeptide Y. *Brain Res* 848: 101–113, 1999.
3. **Chaouloff F, Gunn SH, Young JB.** Central 5-hydroxytryptamine2 receptors are involved in the adrenal catecholamine-releasing and hyperglycemic effects of the 5-hydroxytryptamine indirect agonist D-fenfluramine in the conscious rat. *J Pharmacol Exp Ther* 260: 1008–1016, 1992.
4. **Chaouloff F.** Physiopharmacological interactions between stress hormones and central serotonergic systems. *Brain Res Brain Res Rev* 18: 1–32, 1993.
5. **Ebihara K, Ogawa Y, Katsuura G, Numata Y, Masuzaki H, Satoh N, Tamaki M, Yoshioka T, Hayase M, Matsuoka N, Aizawa-Abe M, Yoshimasa Y, Nakao K.** Involvement of agouti-related protein. An endogenous antagonist of hypothalamic melanocortin receptor, in leptin action. *Diabetes* 48: 2028–2033, 1999.
6. **El-Giamal N, de Zwaan M, Bailer U, Strnad A, Schussler P, Kasper S.** Milnacipran in the treatment of bulimia nervosa: a report of 16 cases. *Eur Neuropsychopharmacol* 13: 73–79, 2003.
7. **Elias CF, Lee CE, Kelly JF, Ahima RS, Kuhar M, Saper CB, Elmquist JK.** Characterization of CART neurons in the rat and human hypothalamus. *J Comp Neurol* 432: 1–19, 2001.
8. **Fan W, Boston BA, Kesterson RA, Hruby VJ, Cone RD.** Role of melanocortinergic neurons in feeding and the agouti obesity syndrome. *Nature* 385: 165–168, 1997.
9. **Fone KC, Topham IA.** Alteration in 5-hydroxytryptamine agonist-induced behaviour following a corticosterone implant in adult rats. *Pharmacol Biochem Behav* 71: 815–823, 2002.
10. **Friedman JM.** Modern science versus the stigma of obesity. *Nat Med* 10: 563–569, 2004.
11. **Gehlert DR, Dreshfield L, Tinsley F, Benvenga MJ, Gleason S, Fuller RW, Wong DT, Hemrick-Luecke SK.** The selective norepinephrine reuptake inhibitor, LY368975, reduces food consumption in animal models of feeding. *J Pharmacol Exp Ther* 287: 122–127, 1998.
12. **Heisler LK, Cowley MA, Tecott LH, Fan W, Low MJ, Smart JL, Rubinstein M, Tatro JB, Marcus JN, Holstege H, Lee CE, Cone RD, Elmquist JK.** Activation of central melanocortin pathways by fenfluramine. *Science* 297: 609–611, 2002.
13. **Kennet GA, Wood MD, Bright F, Trail B, Riley G, Holland V, Avenell KY, Stean T, Upton N, Bromidge S, Forbes IT, Brown AM, Middlemiss DN, Blackburn TP.** SB242084, a selective and brain penetrant 5-HT2C receptor antagonist. *Neuropharmacology* 36: 609–620, 1997.
14. **Laflamme N, Bovetto S, Richard D, Rivest S.** Effect of dexfenfluramine on the transcriptional activation of CRF and its type I receptor within the paraventricular nucleus of the rat hypothalamus. *Br J Pharmacol* 117: 1021–1034, 1996.
15. **Lee MD, Somerville EM, Kennett GA, Dourish CT, Clifton PG.** Tonic regulation of satiety by 5-HT receptors in the mouse: converging evidence from behavioural and c-fos immunoreactivity studies? *Eur J Neurosci* 19: 3017–3025, 2004.
16. **Lee MD, Somerville EM, Kennett GA, Dourish CT, Clifton PG.** Reduced hypophagic effects of D-fenfluramine and the 5-HT2C receptor agonist mCPP in 5-HT1B receptor knockout mice. *Psychopharmacology (Berl)* 176: 39–49, 2004.
17. **Lu D, Willard D, Patel IR, Kadwell S, Overton L, Kost T, Luther M, Chen W, Woychik RP, Wilkison WO, Cone RD.** Agouti protein is an antagonist of the melanocyte-stimulating-hormone receptor. *Nature* 371: 799–802, 1994.
18. **Mochizuki D, Tsujita R, Yamada S, Kawasaki K, Otsuka Y, Hashimoto S, Hattori T, Kitamura Y, Miki N.** Neurochemical and behavioural characterization of milnacipran, a serotonin and noradrenaline reuptake inhibitor in rats. *Psychopharmacology (Berl)* 162: 323–332, 2002.
19. **Nonogaki K, Iguchi A.** Role of central neural mechanisms in the regulation of hepatic glucose metabolism. *Life Sci* 60: 797–807, 1997.
20. **Nonogaki K, Iguchi A.** Stress, acute hyperglycemia, and hyperlipidemia: role of the autonomic nervous system and cytokines. *Trends Endocrinol Metab* 8: 192–197, 1997.
21. **Nonogaki K, Ohashi-Nozue K, Oka Y.** A negative feedback system between brain serotonin systems and plasma active ghrelin levels in mice. *Biochem Biophys Res Commun* 341: 703–707, 2006.
22. **Nonogaki K, Nozue K, Takahashi Y, Yamashita N, Hiraoka S, Kumano H, Kuboki T, Oka Y.** Fluvoxamine, a selective serotonin reuptake inhibitor, and 5-HT2C receptor inactivation induce appetite-suppressing effects in mice via 5-HT1B receptors. *Int J Neuropsychopharmacol* In press.
23. **Nonogaki K, Nozue K, Oka Y.** Hyperphagia alters expression of hypothalamic 5-HT2C and 5-HT1B receptor genes and plasma des-acyl ghrelin levels in A^y mice. *Endocrinology* 147: 5893–5900, 2007.
24. **Puech A, Montgomery SA, Prost JF, Solles A, Briley M.** Milnacipran, a new serotonin and noradrenaline reuptake inhibitor: an overview of its antidepressant activity and clinical tolerability. *Int Clin Psychopharmacol* 12: 99–108, 1997.
25. **Redmond AM, Kelly JP, Leonard BE.** The determination of the optimal dose of milnacipran in the olfactory bulbectomized rat model of depression. *Pharmacol Biochem Behav* 62: 619–623, 1999.
26. **Sugimoto Y, Yamada J, Yoshikawa T, Horisaka K.** Effects of the 5-HT2C/2B receptor agonist 1-(3-chlorophenyl) piperazine on plasma glucose levels of rats. *Eur J Pharmacol* 307: 75–80, 1996.
27. **Tecott LH, Sun LM, Akana SF, Strack AM, Lowenstein DH, Dallman MF, Julius D.** Eating disorder and epilepsy in mice lacking 5-HT2C serotonin receptors. *Nature* 374: 542–546, 1995.
28. **Vickers SP, Clifton PG, Dourish CT, Tecott LH.** Reduced satiating effect of D-fenfluramine in serotonin 5-HT(2C) receptor mutant mice. *Psychopharmacology (Berl)* 143: 309–314, 1999.
29. **Vickers SP, Dourish CT, Kennett GA.** Evidence that hypophagia induced by D-fenfluramine and D-norfenfluramine in the rat is mediated by 5-HT2C receptors. *Neuropharmacology* 41: 200–209, 2001.

0013-7227/07/$15.00/0
Printed in U.S.A.

Endocrinology 148(5):2006–2015

doi: 10.1210/en.2006-1351

Bone Marrow (BM) Transplantation Promotes β-Cell Regeneration after Acute Injury through BM Cell Mobilization

Yutaka Hasegawa,* Takehide Ogihara,* Tetsuya Yamada, Yasushi Ishigaki, Junta Imai, Kenji Uno, Junhong Gao, Keizo Kaneko, Hisamitsu Ishihara, Hironobu Sasano, Hiromitsu Nakauchi, Yoshitomo Oka, and Hideki Katagiri

Division of Advanced Therapeutics for Metabolic Diseases (Y.H., T.O., J.I., K.U., J.G., K.K., H.K.), Center for Translational and Advanced Animal Research, Division of Molecular Metabolism and Diabetes (Y.H., T.Y., Y.I., J.I., K.U., J.G., K.K., H.I., Y.O.), and Department of Pathology (H.S.), Tohoku University Graduate School of Medicine, Sendai 980-8575, Japan; and Laboratory of Stem Cell Therapy (H.N.), Center for Experimental Medicine, Institute of Medical Science, University of Tokyo, Minato-ku, Tokyo 108-8639, Japan

There is controversy regarding the roles of bone marrow (BM)-derived cells in pancreatic β-cell regeneration. To examine these roles *in vivo*, mice were treated with streptozotocin (STZ), followed by bone marrow transplantation (BMT; lethal irradiation and subsequent BM cell infusion) from green fluorescence protein transgenic mice. BMT improved STZ-induced hyperglycemia, nearly normalizing glucose levels, with partially restored pancreatic islet number and size, whereas simple BM cell infusion without preirradiation had no effects. In post-BMT mice, most islets were located near pancreatic ducts and substantial numbers of bromodeoxyuridine-positive cells were detected in islets and ducts. Importantly, green fluorescence protein-positive, *i.e.* BM-derived, cells were detected around islets and were CD45 positive but not insulin positive. Then to examine whether BM-derived cell mobilization contributes to this process, we used *Nos3*$^{-/-}$ mice as a model of impaired BM-derived cell mobilization. In streptozotocin-treated *Nos3*$^{-/-}$ mice, the effects of BMT on blood glucose, islet number, bromodeoxyuridine-positive cells in islets, and CD45-positive cells around islets were much smaller than those in streptozotocin-treated *Nos3*$^{+/+}$ controls. A series of BMT experiments using *Nos3*$^{+/+}$ and *Nos3*$^{-/-}$ mice showed hyperglycemia-improving effects of BMT to correlate inversely with the severity of myelosuppression and delay of peripheral white blood cell recovery. Thus, mobilization of BM-derived cells is critical for BMT-induced β-cell regeneration after injury. The present results suggest that homing of donor BM-derived cells in BM and subsequent mobilization into the injured periphery are required for BMT-induced regeneration of recipient pancreatic β-cells. (*Endocrinology* 148: 2006–2015, 2007)

SEVERAL LINES OF evidence indicate that bone marrow (BM)-derived cells are capable of transdifferentiating into various cell types, including endothelial cells, arterial smooth muscle cells, myoblasts, myocardium, and epithelia of the gastrointestinal tract (1–6). In the field of regenerative medicine for diabetes treatment, BM cells are seen as promising pancreatic β-cell sources (7–9). However, whether BM cells can transdifferentiate into β-cells and/or stimulate β-cell differentiation is controversial.

A previous study (10) showed that BM-derived cells can directly transdifferentiate into β-cells. In that report, 4–6 wk after BM transplantation (BMT; *i.e.* lethal irradiation of recipient mice and subsequent BM cell infusion from other mice), donor BM-derived insulin-positive cells were detected in 1.7–3% of pancreatic islet cells. However, in subsequent similar studies (11–13), very few or no donor BM-derived insulin-positive cells were detected in recipient islets, suggesting that if direct transdifferentiation from BM-derived cells into β-cells occurs, it would involve only a very small percentage of cells. BM-derived cells also reportedly initiate recipient β-cell regeneration rather than directly transdifferentiating into β-cells (14). In that study, BMT increased recipient β-cells with the appearance of donor-derived endothelial cells in the pancreas, resulting in improvement of hyperglycemia in streptozotocin (STZ)-induced diabetic mice. Other studies also demonstrated that BMT improves hyperglycemia in diabetic animals such as STZ-treated mice (15) and rats (16), E2f1/E2f2 mutant mice (17), and KKAy mice (18). However, several studies obtained contradictory results, *i.e.* no improvement in hyperglycemia after BMT (12, 19). Whether BMT promotes β-cell regeneration and improves hyperglycemia in diabetic mice and, if so, how β-cells are regenerated remains essentially unknown. Herein we attempted to address these questions.

First, we observed that BMT, but not simple BM cell infusion without preirradiation, restored islet numbers and improved hyperglycemia in STZ-treated mice. Donor-derived cells were detected around post-BMT islets and were

First Published Online January 25, 2007

* Y.H. and T.O. contributed equally to this work.

Abbreviations: BM, Bone marrow; BMT, BM transplantation; BrdU, bromodeoxyuridine; eNOS, endothelial nitric oxide synthase; FACS, fluorescence-activated cell sorting; FITC, fluorescein isothiocyanate; GFP, green fluorescence protein; MMP, matrix metalloproteinase; PECAM, platelet endothelial cell adhesion molecule; sKitL, soluble kit-ligand; STZ, streptozotocin; WBC, white blood cell.

Endocrinology is published monthly by The Endocrine Society (http://www.endo-society.org), the foremost professional society serving the endocrine community.

CD45 (pan-hematopoietic marker) positive, suggesting that mobilization of BM-derived cells to the pancreas induces β-cell regeneration. To examine this hypothesis, we performed BMT experiments using endothelial nitric oxide synthase (eNOS)-deficient ($Nos3^{-/-}$) mice, in which mobilization of BM-derived cells after myelosuppression is impaired (20). In STZ-treated $Nos3^{-/-}$ mice, BMT effects on β-cell regeneration and improvement of hyperglycemia were very limited. Thus, BM-derived cell mobilization is apparently involved in BMT-induced β-cell regeneration after acute injury.

Materials and Methods

Animals

C57BL/6J mice were purchased from Clea Japan, Inc. (Tokyo, Japan). Green fluorescent protein (GFP) transgenic mice with the C57BL/6J background were kindly provided by Dr. M. Okabe (Osaka University, Osaka, Japan) (21). Enhanced GFP is under transcriptional control of the chicken β-actin promoter and the cytomegalovirus enhancer in this strain, resulting in high-level expression in most tissues. $Nos3^{-/-}$ mice were purchased from Jackson Laboratories (Bar Harbor, ME). Age- and sex-matched wild-type ($Nos3^{+/+}$) littermates served as controls. These animals were generated and have been maintained with a C57BL/6J background by backcrossing of hemizygous carriers to C57BL/6J for more than six generations. Mice were housed in an air-conditioned environment, with a 12-h light, 12-h dark cycle, and fed a regular unrestricted diet. Hyperglycemia was induced by ip infusion of 35 mg/kg body weight STZ (Sigma-Aldrich, St. Louis, MO) daily for 8 d [modification of method reported by Wang *et al.* (22)]. STZ was solubilized in citrate sodium buffer (pH 4.5) and injected, within 15 min after preparation, into 6-wk-old mice. All animal experiment procedures were approved by our Institutional Review Board, Tohoku University School of Medicine, and conducted according to institutional guidelines for animal experiments.

Measurements

Blood glucose was measured after a 10-h fast and assayed using Antsense II (Horiba Industry, Kyoto, Japan). Plasma insulin was determined with an ELISA kit (Morinaga Institute of Biological Science, Yokohama, Japan). Insulin content was measured as described previously (23).

BMT

BM cells were flushed in bulk from the medullary cavities of femurs and tibias. BM donors were young (6 wk old) sex-matched GFP transgenic mice and $Nos3^{-/-}$ or $Nos3^{+/+}$ mice. Recipient mice were lethally irradiated (10 Gy) and reconstituted a single iv infusion of 2×10^6 BM cells, from donor mice through the tail vein. Tissues were analyzed 30–40 d after BMT. The percentage of GFP-positive cells among recipient BM cells was determined by fluorescence-activated cell sorting (FACS), using a FACS Caliber with CellQuest software (BD PharMingen, Franklin Lakes, NJ).

Bromodeoxyuridine (BrdU) in situ detection

To identify proliferating cells in the pancreas, BrdU was injected according to the BrdU *in situ* detection kit protocol (BD Bioscience, San Jose, CA). Mice were injected ip with 1 mg BrdU 24 h before pancreas extraction at 0, 3, 7, 10, 15, or 25 d after BMT. The labeled cells were immunostained with anti-BrdU antibody. To calculate numbers of islets and cells per islet and the percentage of BrdU-positive cells among islet cells, we microscopically examined the whole pancreas in 30-μm sections and counted the numbers of islets, islet cells, and BrdU-positive nuclei in islets.

Immunohistochemistry

Mouse pancreases were excised and fixed overnight in 10% paraformaldehyde. Fixed tissues were processed for paraffin embedding and 3-μm sections were prepared. The streptavidin-biotin method was performed with a Histofine streptavidin-biotin-PO kit (Nichirei, Tokyo, Japan) for immunostaining using antibody against insulin (Sigma-Aldrich) or GFP (Santa Cruz Biotechnology, Santa Cruz, CA). Slides were deparaffinized and immediately exposed to the blocking solution. Sections were incubated for 18 h at 4 C with antibody against human insulin or GFP diluted 1:1000 in PBS. Slides were incubated with the biotinylated IgG for 1 h and then peroxidase-conjugated streptavidin for 30 min at room temperature. Finally, immunoreactivity was visualized by incubation with a substrate solution containing 3,3′-diaminobenzidine tetrahydrochloride. For double staining of insulin and BrdU, the streptavidin-peroxidase method was applied, followed by incubation with Simple stain 3-amino-9-ethyl carboxazole solution (Nichirei).

Fluorescent immunohistochemistry

For double staining of insulin with glucagon, keratin/cytokeratin, or CD45, the 3-μm sections of paraffin-embedded pancreases were incubated overnight with the respective antibodies at 4 C. Antibodies against insulin, glucagon (Dako Corp., Carpinteria, CA), keratin/cytokeratin (Nichirei, and CD45 (Santa Cruz Biotechnology) were diluted 1:1000 in PBS. For platelet endothelial cell adhesion molecule (PECAM)-1 staining, sections were immunostained with rat anti-CD31 (1:10; BD Biosciences). Labeled cells were visualized with a biotin-conjugated secondary antibody with streptavidin, TX red conjugate (Vector Laboratories, Burlingame, CA). For double staining of insulin with glucagon or keratin/cytokeratin, the sections were incubated for 1 h at room temperature in a mixture of Alexa Fluor 488 goat chicken antimouse IgG (Molecular Probes, Eugene, OR) diluted 1:100 and Alexa Fluor 594 donkey antirabbit diluted 1:50 in PBS. For double staining of insulin and CD45, the sections were incubated in a mixture of Alexa Fluor 488 chicken antimouse IgG and Alexa Fluor 546 goat antirabbit IgG diluted 1:1000 in PBS. Sections were observed under a fluorescence microscope, LSM 5 PASCAL (Carl Zeiss, Oberkochen, Germany) and the image was analyzed using the PASCAL system.

Statistical analysis

Data are expressed as means ± SE. Differences between experimental groups were evaluated using the unpaired Student's t test for several independent observations. $P < 0.05$ was considered significant.

Results

Recipient BM was replaced with donor cells after irradiation followed by BM cell infusion but not after simple BM cell infusion without preirradiation

Six-week-old C57BL/6J mice were given STZ daily for 8 d, followed by lethal irradiation and subsequent infusion of BM cells (STZ+BMT mice). In these experiments, BM cells were obtained from GFP transgenic mice (Fig. 1A). A group of STZ-treated mice was simply infused with the same number (2×10^6) of BM cells without preirradiation (STZ+BM-infused mice). First, we confirmed replacement of recipient BM with that of donor mice using fluorescence microscopy and FACS analysis. As shown in Fig. 1B, there were no GFP-positive cells in the BM of C57BL/6J mice, whereas nearly all BM cells from GFP mice were GFP positive. BM cells of STZ+BMT mice showed high donor chimerism, indicating the recipient BM to have essentially been replaced with donor BM cells. In contrast, STZ+BM-infused mice had no donor-derived GFP cells in their BM, suggesting that preirradiation is necessary for BM replacement.

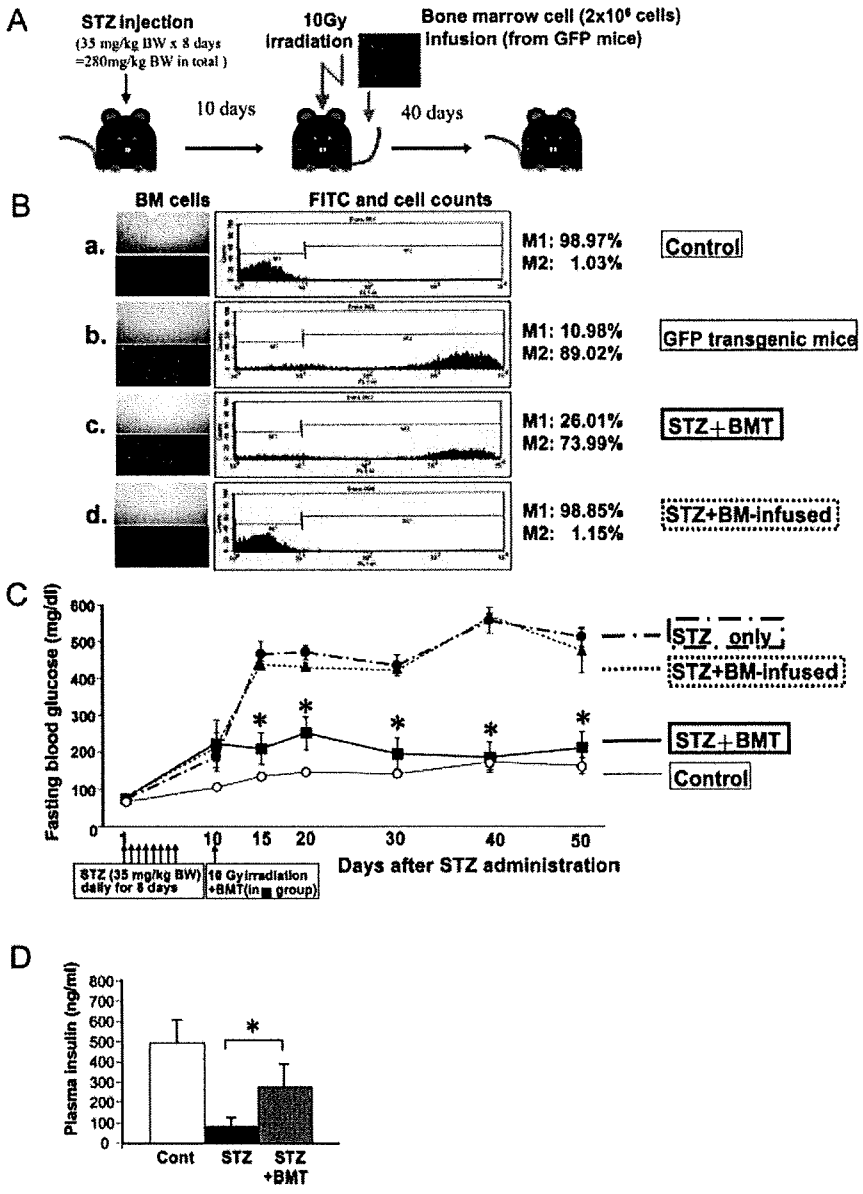

FIG. 1. BMT in STZ-treated mice. A, Experimental protocol. B, Bone marrow chimerism. Bright field (*left upper panels*), FITC (*left lower panels*), and representative FACS analyses of bone marrow chimerism from C57BL/6J mice (a), GFP transgenic mice (b), STZ-treated mice receiving lethal irradiation and BMT from GFP transgenic mice (c), and STZ-treated mice infused with BM cells of GFP transgenic mice, without preirradiation (d) (*right panels*) are shown. C, Fasting blood glucose of STZ-treated mice with or without BMT. ▲, STZ-treated mice without BMT (hyperglycemic control); ■, STZ-treated mice receiving BMT (lethal irradiation and subsequent BM cell infusion from GFP transgenic mice); ●, STZ-treated mice infused with BM cells of GFP transgenic mice, without preirradiation; ○, mice with neither STZ nor BMT (normoglycemic control). *, $P < 0.05$ for ■, compared with ▲ group (n = 5–6 in each group). D, Fasting plasma insulin on d 40. Cont, Mice with neither STZ nor BMT (normoglycemic control); STZ, STZ-treated mice without BMT (hyperglycemic control); STZ+BMT, STZ-treated mice receiving BMT. *, $P < 0.05$ for STZ+BMT, compared with STZ group (n = 5–6 in each group).

BMT, but not simple BM cell infusion without preirradiation, improved hyperglycemia in STZ-treated mice

As shown in Fig. 1C, STZ-treated mice receiving neither irradiation nor BM cell infusion (hyperglycemic controls) showed markedly higher fasting blood glucose than mice without STZ treatment (normoglycemic controls). Notably, blood glucose levels of STZ+BMT mice were significantly lower than those of hyperglycemic controls. Forty days after the first STZ administration, blood glucose levels of STZ+BMT mice were similar to those of normoglycemic controls. However, blood glucose levels of STZ+BM-infused mice did not decrease, instead remaining similar to those of hyperglycemic controls for 50 d after STZ administration. We additionally examined the effects of BMT, performed 30 d after STZ treatment. This late BMT did not significantly decrease blood glucose levels (supplemental Fig. 1, published as supplemental data on The Endocrine Society's Journals Online web site at http://endo.endojournals.org). Together, these findings suggest that BMT improves hyperglycemia after acute injury of pancreatic β-cells with STZ treatment.

Next, we measured fasting plasma insulin levels on d 40 (Fig. 1D) in STZ+BMT mice. STZ administration markedly decreased plasma insulin levels, whereas BMT partially but significantly restored these levels by d 40.

STZ administration followed by BMT increased pancreatic islets in the vicinity of pancreatic ducts

We histologically analyzed pancreatic islets in the four groups. With hematoxylin-eosin staining on d 35, islet number and size were markedly decreased in hyperglycemic (Fig. 2A, b and f), as compared with normoglycemic (Fig. 2A, a and e), controls. Whereas simple BM infusion without preirradiation did not reverse the diminished number and size of

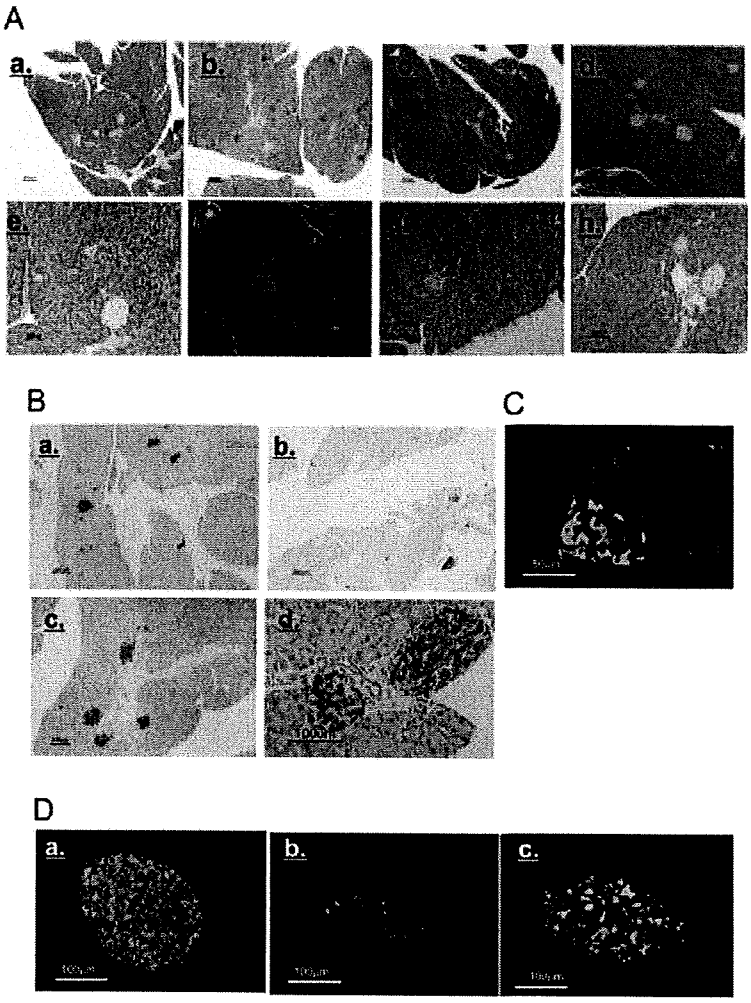

FIG. 2. Pancreatic islets of STZ-treated mice receiving subsequent BMT. A, Hematoxylin-Eosin staining of pancreases on d 35. Pancreases from normoglycemic control mouse (a and e), hyperglycemic control mouse (b and f), STZ-treated mouse simply infused with BM cells without preirradiation (c and g), and STZ-treated mouse receiving lethal irradiation and BMT (d and h). a–d, Magnification, ×40; e–h, ×100. B, Antiinsulin immunostaining of pancreases. Pancreases from normoglycemic control mouse (a), hyperglycemic control mouse (b), and STZ-treated mouse receiving BMT (c and d). a–c, Magnification, ×40; d, ×200. C, Double immunostaining of pancreas with antiinsulin and antikeratin/cytokeratin antibodies. *Green* indicates insulin-positive and *red* keratin/cytokeratin-positive cells, *i.e.* pancreatic ductal epithelium. D, Double immunostaining of pancreases with antiinsulin and antiglucagon antibodies. Pancreases from normoglycemic control mouse (a), hyperglycemic control mouse (b), and STZ-treated mouse receiving BMT (c). In C and D, to avoid overlapping staining of GFP with FITC, BM cells obtained from wild-type C57BL/6J mice, but not from GFP transgenic mice, were transplanted. Representative histological findings among six independent experiments are presented.

islets (Fig. 2A, c and g), islet number and size were both restored in STZ+BMT mice (Fig. 2A, d and h). Several islet populations were enlarged as compared with those in normoglycemic controls (Fig. 2A, a and e *vs.* d and h).

Antiinsulin staining of pancreatic specimens is shown in Fig. 2B. In hyperglycemic controls, insulin-positive cells were markedly diminished (Fig. 2B, b) as compared with normoglycemic controls (Fig. 2B, a). In contrast, in STZ+BMT mice, islet numbers were restored and sizes varied with some being enlarged (Fig. 2B, c). Notably, in the large view (Fig. 2B, d), a major population of insulin-positive cells in STZ+BMT mice is located in the vicinity of pancreatic ducts, which were stained with antikeratin/cytokeratin antibody (Fig. 2C).

Next, we performed double immunostaining using antibodies against insulin and glucagon. In immunofluorescent experiments (Figs. 2, C and D), to avoid overlapping staining of GFP with fluorescein isothiocyanate (FITC), BM cells obtained from wild-type C57BL/6J mice, but not GFP transgenic mice, were transplanted. Compared with islets of normal and STZ-treated mice (Fig. 2D, a and b), islets in STZ+BMT mice exhibited normal architecture with slightly fewer β-cells surrounded by α-cells (Fig. 2D, c).

To exclude the possibility that irradiation suppresses inflammation in response to STZ and prevents β-cell injury, STZ-treated mice were exposed to lethal irradiation (10 Gy) without subsequent BM cell infusion. Lethal irradiation alone did not lower blood glucose in STZ-treated mice. Pancreatic islets were diminished in size, as in hyperglycemic controls, 9 d after irradiation (mice died 10–14 d after lethal irradiation without BMT in our experiment; data not shown). Next, to examine prolonged effects of irradiation, mice were sublethally irradiated (5 Gy). Sublethal irradiation alone likewise did not significantly improve hyperglycemia in STZ-treated mice (data not shown), suggesting that irradiation does not exert protective effects against STZ-induced β-cell injury.

To further examine whether these islets in STZ+BMT mice were regenerated or only protected from STZ injury, BrdU staining was performed. In islets of normoglycemic (Fig. 3A) and hyperglycemic (Fig. 3B) controls, there were very few BrdU-positive cells. In contrast, islets of STZ+BMT mice (10 d after BMT) contained substantial numbers of BrdU-positive cells in and around islets, and some were detected among the pancreatic ductal cells (Fig. 3C). In other sections as well, islets containing BrdU-positive cells were mostly located near ducts and blood vessels. Most BrdU-positive cells in islets were insulin positive, whereas those outside the islets, mostly in the ductal structure, did not express insulin.

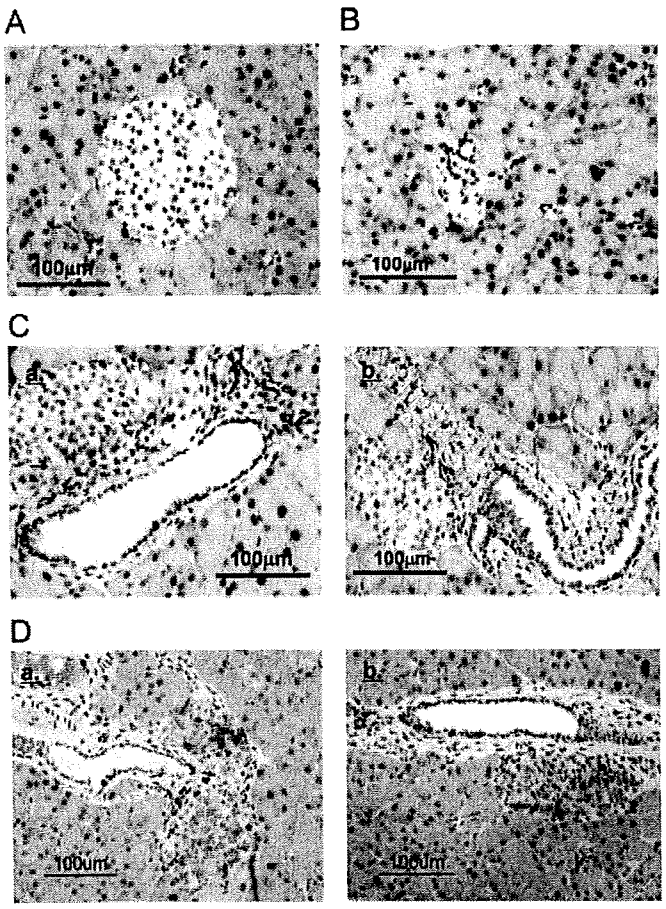

FIG. 3. BrdU-positive proliferating cells in pancreases of STZ-treated mice receiving subsequent BMT. A–C, Pancreases from normoglycemic control mouse (A), hyperglycemic control mouse (B), and STZ-treated mice receiving BMT (C) (10 d after BMT). *Brown cells* are BrdU positive. D, Double immunostaining of pancreases from STZ-treated mice receiving BMT (10 d after BMT) with antiinsulin and anti-BrdU. *Brown* and *red cells* are BrdU and insulin positive, respectively.

(Fig. 3D). Given reports that pancreatic stem/progenitor cells exist among ductal cells (24–26), BMT after STZ treatment might stimulate the generation of new islets from ductal progenitor cells as well as proliferation of β-cells in this model.

We also quantitatively examined the time courses of islet numbers, cell number per islet and percentage of BrdU-positive cells among islet cells after BMT (Table 1). Although decreased by STZ, islet number was significantly increased 10 and 15 d after BMT. The peak islet number was greater than in normoglycemic control mice by 47%. The islet number and percentage of BrdU-positive cells among islet cells were also increased through 10 d after BMT and then fell to normoglycemic control levels. These findings clearly indicate that BMT induces β-cell regeneration, resulting in pancreatic islet restoration in this model.

Although no BM-derived insulin-positive cells were detected, the regenerated islets were surrounded by BM-derived CD45-positive cells

To investigate whether BM-derived cells transdifferentiated into insulin-producing cells in our model, pancreases from STZ+BMT mice on d 35 were immunostained with antiinsulin antibody, followed by an intensive search for both insulin- and GFP-positive cells using confocal fluorescence microscopy. However, no double-positive cells were detected (Fig. 4A), suggesting that regenerated β-cells in STZ+BMT mice are derived from recipient cells. In contrast, intriguingly, GFP-positive, *i.e.* BM-derived, cells were located around islets (Fig. 4A). In STZ+BM-infused mice, no GFP-positive cells were detected around islets (data not shown). Immunostaining with anti-GFP antibody confirmed that GFP-positive cells exist around islets of STZ+BMT mice (Fig. 4B, *black arrows* indicate islets). To identify the lineage of BM-derived cells around islets, we used several antibodies to immunostain lineage markers. GFP-positive cells around islets were CD45-positive (Fig. 4C, *white arrows* indicate islets), although these cells were not positively stained with F4/80, CD68 (macrophage lineage), CD3/CD5 (T cell lineage), or CD20 (B cell lineage) (data not shown), suggesting immature hematopoietic cells. We additionally examined whether these BM-derived cells are positive for an endothelial cell marker, CD31 (PECAM-1). Although a few GFP-positive cells were positive for CD 31 (Fig. 4D, *red arrow*), most BM-derived cells in or around islets were not positively stained with this endothelial marker. Taken together, these observations suggest that donor immature hematopoietic cells, which may be expanded and mobilized to peripheral blood after BMT, initiate β-cell regeneration.

Mobilization of BM-derived cells is necessary for the glucose-lowering effect of BMT after STZ administration

To determine whether BM-derived cell mobilization is pivotal in this process, we investigated the effects of BMT on

TABLE 1. Islet numbers and BrdU-positive cells per pancreatic islet cells of STZ-treated mice receiving subsequent BMT

	Days after BMT	Nos. of islets	Nos. of BrdU-positive cells	Nos. of cells in islets	Percentage of BrdU-positive cells among islet cells
STZ(−) control		94.0 ± 17.3	33.3 ± 4.5	7174 ± 1487	0.51 ± 0.08
	0	62.0 ± 11.9	20.6 ± 5.6	4658 ± 1019	0.47 ± 0.11
	3	48.3 ± 2.0	40.7 ± 16.2	2974 ± 278	1.41 ± 0.51
STZ+BMT (days after BMT)	7	102.7 ± 11.6	194.3 ± 33.4[a]	6159 ± 528	3.10 ± 0.31[a]
	10	138.0 ± 22.9[a]	253.0 ± 107.8[a]	7989 ± 756[a]	3.40 ± 1.63
	15	113.7 ± 6.9[a]	64.7 ± 16.3	5223 ± 539	1.34 ± 0.40
	25	82.0 ± 6.4	37.5 ± 0.4	3953 ± 157	0.95 ± 0.03

To calculate numbers of islets and cells per islet and the percentage of BrdU-positive cells among islet cells, we microscopically examined the whole pancreas in 30-μm sections and counted the numbers of islets, islet cells, and BrdU-positive nuclei in islets.

[a] $P < 0.05$ *vs.* d 0 in STZ+BMT group.

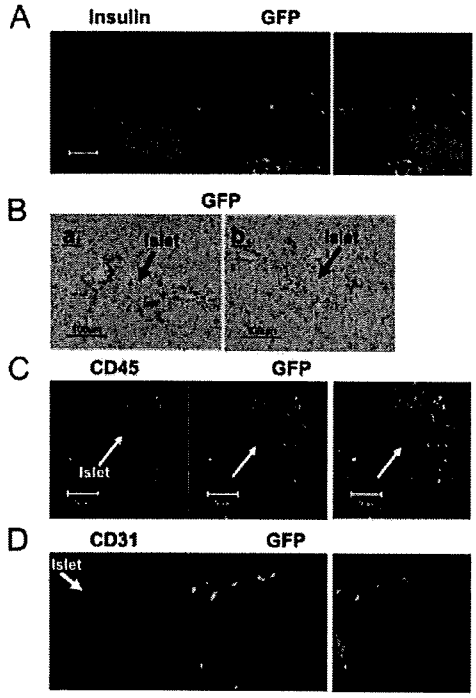

FIG. 4. BM-derived cells in pancreases of STZ-treated mice receiving subsequent BMT. A, BM-derived cells and insulin-positive cells in pancreas of STZ-treated mouse receiving BMT from GFP transgenic mice. Pancreases of STZ-treated mouse receiving subsequent BMT from GFP transgenic mice (35 d after the first STZ). *Left panel*, Insulin-positive cells; *middle panel*, GFP-positive, *i.e.* BM-derived cells; *right panel*, merged image of the *left* and *middle panels*. B, BM-derived cells in pancreases of STZ-treated mice receiving BMT from GFP transgenic mice. *Brown cells* are GFP positive, *i.e.* BM-derived cells, and *arrows* indicate islets. C, CD45-positive and BM-derived cells in pancreas of STZ-treated mice receiving BMT from GFP transgenic mice. *Left panel*, Immunostaining with anti-CD45 antibody. *Red* indicates CD45-positive cells. *Middle panel*, *Green* indicates GFP-positive cells. *Right panel*, Merged image of the *left* and *middle panels*. *Yellow* indicates GFP and CD45 double-positive cells. *Arrows* indicate islets. D, CD31 (PECAM-1)-positive and BM-derived cells in pancreases of STZ-treated mice receiving BMT from GFP transgenic mice. *Left panel*, Immunostaining with anti-CD31 antibody. *Red* indicates CD31-positive cells. *Middle panel*, *Green* indicates GFP-positive cells. *Right panel*, Merged image of *left* and *middle panels*.

β-cell regeneration using eNOS-deficient ($Nos3^{-/-}$) mice as a model for impaired BM-derived cell mobilization. In $Nos3^{-/-}$ mice, mobilizations of hematopoietic stem cells and endothelial progenitor cells from BM were reportedly impaired after myelosuppression. Deficiency in eNOS reportedly reduces hematopoietic recovery in response to 5-fluorouracil treatment due to impaired progenitor cell mobilization (20). Therefore, we performed similar experiments using $Nos3^{-/-}$ mice. First, we compared two BMT groups, *i.e.* $Nos3^{+/+}$ donors to $Nos3^{+/+}$ recipients ($Nos3^{+/+}$ *to* $Nos3^{+/+}$ mice) and $Nos3^{-/-}$ donors to $Nos3^{-/-}$ recipients ($Nos3^{-/-}$ to $Nos3^{-/-}$ mice).

Peripheral white blood cells (WBCs) were counted after lethal irradiation and subsequent BM infusion (Fig. 5A). Myelosuppression after irradiation was profound and recovery of peripheral WBC counts was markedly delayed in $Nos3^{-/-}$ to $Nos3^{-/-}$ mice *vs.* $Nos3^{+/+}$ to $Nos3^{+/+}$ mice. Thus, eNOS deficiency impairs hematopoietic reconstitution after not only 5-fluorouracil treatment but also BMT. We measured the blood glucose levels after STZ administration followed by BMT (Fig. 5B). In $Nos3^{+/+}$ to $Nos3^{+/+}$ mice, STZ-induced hyperglycemia was improved to nearly normoglycemic control levels 40 d after the first STZ administration, consistent with the findings shown in Fig. 1C. In contrast, in $Nos3^{-/-}$ to $Nos3^{-/-}$ mice, BMT did not improve STZ-induced hyperglycemia (Fig. 5B). Thus, eNOS function is essential for improving hyperglycemia after BMT.

In $Nos3^{-/-}$ to $Nos3^{-/-}$ mice, not only mobilization of BMT-derived progenitor cells but also pancreatic endothelial function may be impaired due to systemic eNOS deficiency. Therefore, we performed an additional BMT, *i.e.* $Nos3^{-/-}$ donors to $Nos3^{+/+}$ recipients ($Nos3^{-/-}$ to $Nos3^{+/+}$ mice), whose eNOS is intact in pancreatic blood vessels. In $Nos3^{-/-}$ to $Nos3^{+/+}$ mice, myelosuppression was profound and subsequent recovery of the WBC count was delayed, compared with $Nos3^{+/+}$ to $Nos3^{+/+}$ mice, but this delay in recovery was significantly less severe than that seen in $Nos3^{-/-}$ recipients (Fig. 5A). In $Nos3^{-/-}$ to $Nos3^{+/+}$ mice, blood glucose levels also reached midrange values; the glucose-lowering effects of BMT did occur but were significantly blunted (Fig. 5B). These findings indicate that the lack of hyperglycemia improvement in $Nos3^{-/-}$ to $Nos3^{-/-}$ mice is not attributable solely to the impaired pancreatic endothelial function of recipients. The glucose-lowering effect of BMT inversely correlates with the severity of myelosuppression and delayed recovery, which apparently reflects impaired mobilization of BM cells to peripheral blood.

BMT-induced β cell regeneration was impaired in STZ-treated $Nos3^{-/-}$ mice

To quantify BMT-induced β-cell regeneration in $Nos3^{+/+}$ to $Nos3^{+/+}$ and $Nos3^{-/-}$ to $Nos3^{-/-}$ mice, pancreatic insulin contents 40 d after STZ (30 d after BMT) were measured (Fig. 5C). Compared with $Nos3^{+/+}$ controls without STZ treatment, STZ-treated $Nos3^{+/+}$ mice had markedly lower pancreatic insulin contents. In $Nos3^{+/+}$ to $Nos3^{+/+}$ mice, BMT partially restored pancreatic insulin contents, consistent with our findings that plasma insulin levels were partially restored by BMT (Fig. 1D). In contrast, in $Nos3^{-/-}$ to $Nos3^{-/-}$ mice, BMT effects on pancreatic insulin contents were very limited; pancreatic insulin contents were significantly lower in $Nos3^{-/-}$ to $Nos3^{-/-}$ mice than in $Nos3^{+/+}$ to $Nos3^{+/+}$ mice (Fig. 5C).

Next, changes in islet numbers and percentage of BrdU-positive cells among islet cells in response to BMT were compared between $Nos3^{+/+}$ to $Nos3^{+/+}$ mice and $Nos3^{-/-}$ to $Nos3^{-/-}$ mice. Whereas islet numbers were increased in STZ-treated $Nos3^{+/+}$ to $Nos3^{+/+}$ mice during the period 7–15 d after BMT, islet numbers were significantly less in STZ-treated $Nos3^{-/-}$ to $Nos3^{-/-}$ mice (Fig. 5D). In addition, whereas percentages of BrdU-positive cells among islet cells were markedly increased in STZ-treated $Nos3^{+/+}$ to $Nos3^{+/+}$ mice 7–10 d after BMT, there were significantly fewer such cells in STZ-treated $Nos3^{-/-}$ to $Nos3^{-/-}$ mice (Fig. 5E). These results suggest that impaired BM-derived cell mobilization

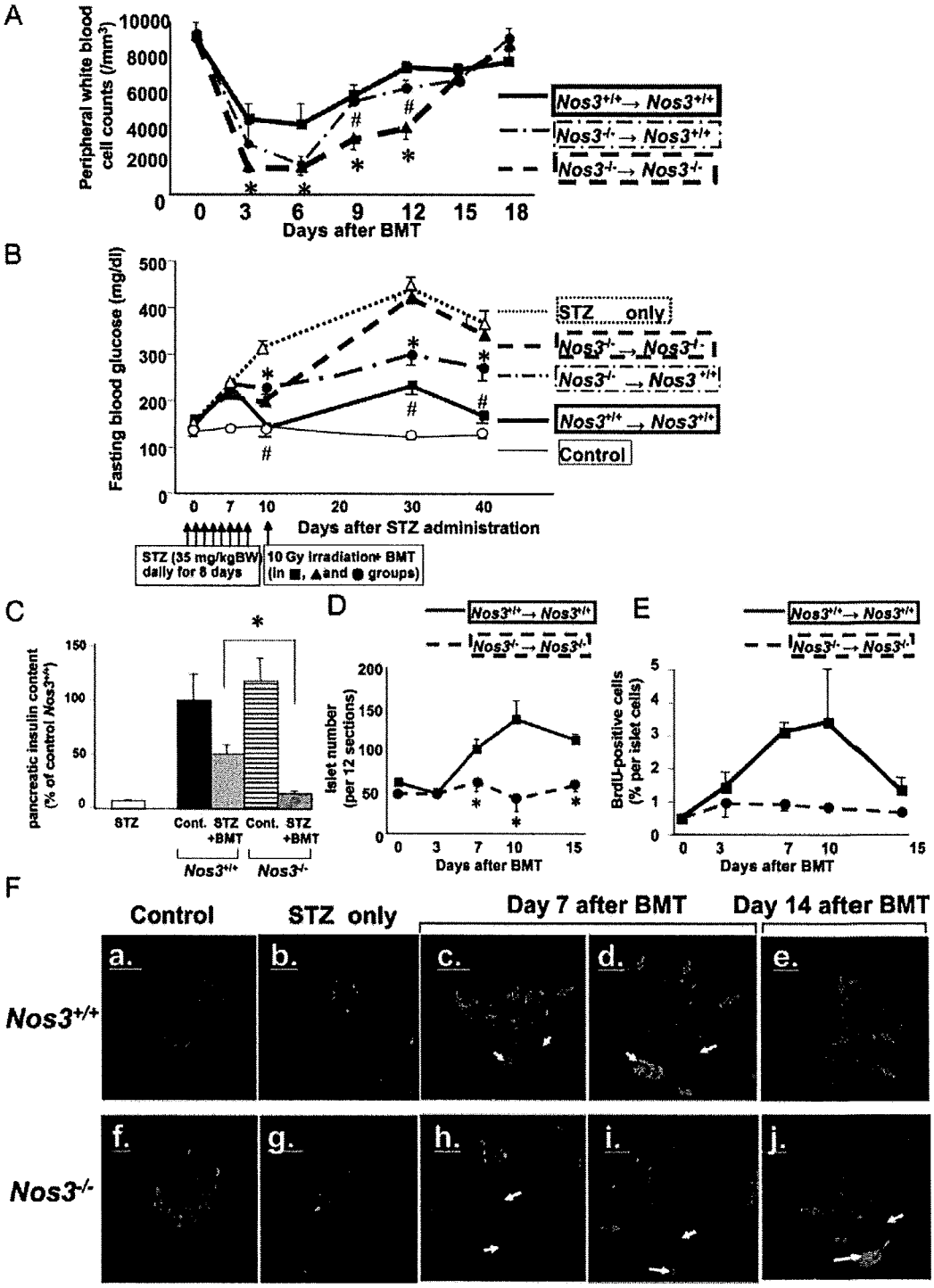

FIG. 5. BMT experiments using $Nos3^{+/+}$ and $Nos3^{-/-}$ mice. A, Time courses of peripheral WBC counts in $Nos3^{+/+}$ and $Nos3^{-/-}$ mice receiving BMT. ■, STZ-treated $Nos3^{-/+}$ mice receiving BMT from $Nos3^{+/+}$ mice; ▲, STZ-treated $Nos3^{-/-}$ mice receiving BMT from $Nos3^{-/-}$ mice; ●, STZ-treated $Nos3^{+/+}$ mice receiving BMT from $Nos3^{-/-}$ mice. *, $P < 0.05$ for ▲, compared with ■ group; #, $P < 0.05$ for ●, compared with ▲ group, respectively (n = 5–6 in each group). B, Fasting blood glucose levels of $Nos3^{+/+}$ and $Nos3^{-/-}$ receiving BMT. ○, Normoglycemic control $Nos3^{+/+}$ mice with neither STZ nor BMT; △, STZ-treated $Nos3^{+/+}$ mice without BMT (hyperglycemic control); ■, STZ-treated $Nos3^{+/+}$ mice receiving BMT from $Nos3^{+/+}$ mice; ▲, STZ-treated $Nos3^{-/-}$ mice receiving BMT from $Nos3^{-/-}$ mice; ●, STZ-treated $Nos3^{+/+}$ mice receiving BMT from $Nos3^{-/-}$ mice. *, $P < 0.05$ for ●, compared with △ group; # $P < 0.05$ for ■, compared with ● group, respectively (n = 5–6 in each group). C, Pancreatic insulin contents. STZ, STZ-treated $Nos3^{+/+}$ mice without BMT; Cont, $Nos3^{+/+}$ or $Nos3^{-/-}$ mice with neither STZ nor BMT; STZ+BMT, STZ-treated $Nos3^{+/+}$ mice receiving BMT from $Nos3^{+/+}$ mice and STZ-treated $Nos3^{-/-}$ mice receiving BMT from $Nos3^{-/-}$ mice. *, $P < 0.05$ between STZ-treated $Nos3^{+/-}$ mice receiving BMT from $Nos3^{+/+}$ mice and STZ-treated $Nos3^{-/-}$ mice receiving BMT from $Nos3^{-/-}$mice. D, Time courses of islet numbers after BMT. E, Time courses of BrdU-positive cell percentage per islet cells after BMT. In D and

in *Nos3*$^{-/-}$ mice suppresses BMT-induced β-cell regeneration after acute injury.

BM-derived CD45-positve cells around islets are important for β-cell regeneration-induced by BMT

To examine whether impaired mobilization of BM-derived cells in *Nos3*$^{-/-}$ mice affects hematopoietic cell assembly around islets and β-cell regeneration, we compared pancreases from *Nos3*$^{+/+}$ to *Nos3*$^{+/+}$ and *Nos3*$^{-/-}$ to *Nos3*$^{-/-}$ mice using antiinsulin and CD45 antibodies (Fig. 5F). In *Nos3*$^{+/+}$ to *Nos3*$^{+/+}$ mice, substantial numbers of CD45-positive cells were detected in and around the regenerated islets (*red arrows* in Fig. 5F, c–e). No such cells were detected around islets in *Nos3*$^{+/+}$ or *Nos3*$^{-/-}$ mice treated with STZ alone (Fig. 5F, b and g), suggesting that STZ-induced inflammation alone is not responsible for recruiting these cells. In pancreases from *Nos3*$^{+/+}$ to *Nos3*$^{+/+}$ mice, regenerated islets were located near pancreatic ducts and blood vessels (*white arrows* in Fig. 5F, c–e). In contrast, β-cell regeneration was markedly impaired in *Nos3*$^{-/-}$ to *Nos3*$^{-/-}$ mice (Fig. 5F, h–j), and far fewer CD45-positive cells were present in and around islets in *Nos3*$^{-/-}$ to *Nos3*$^{-/-}$ than in *Nos3*$^{+/+}$ to *Nos3*$^{+/+}$ mice. These results support the notion that BMT-induced BM-derived cell mobilization is critical for regeneration of recipient β-cells from stem/progenitor cells in pancreatic ducts.

Discussion

Recently considerable research attention has focused on pancreatic β-cell regeneration. In particular, several previous studies examined the role of BM-derived cells in β-cell regeneration using BMT (10–18), but no definitive conclusions have yet been reached. In this study, we clearly demonstrate that BMT can regenerate recipient β-cells under certain conditions. Our data supported those of a previous report (14) showing BMT to improve hyperglycemia in STZ-induced diabetic mice via regeneration of recipient pancreatic β-cells. Herein we attempted to elucidate the mechanisms whereby BMT induces β-cell regeneration.

First, we demonstrated that BMT, but not simple BM cell infusion without preirradiation, promotes β-cell regeneration after STZ-induced injury. What are the differences between these procedures? BMT involves lethal irradiation and subsequent BM cell infusion. We confirmed, using FACS analysis, that recipient BM is essentially replaced with that of donor mice after BMT. In contrast, mice receiving BM cell infusion alone without preirradiation showed no BM replacement with donor-derived cells. Myelosuppression and subsequent expansion of donor BM cells take place in BMT. During this process, donor BM cells home to the BM microenvironment and progenitor cells mobilize and expand in the peripheral blood (27). In contrast, simple BM cell infusion does not induce homing or expansion of donor BM cells. Therefore, expansion of immature BM cells, which are rarely detected in peripheral blood in normal circumstances, is likely to be important for β-cell regeneration after BMT. We ruled out the possibility that irradiation suppresses inflammation in response to STZ administration and prevents β-cell injury. STZ-treated mice were exposed to lethal (10 Gy) and sublethal (5 Gy) irradiation without subsequent BM cell infusion. Irradiation alone had no effect on hyperglycemia or β-cell number in STZ-treated mice. Furthermore, in STZ+BMT mice on d 2 after BMT, islet numbers and cell numbers per islet were both significantly decreased by STZ but were restored by d 10. Thus, it is unlikely that irradiation itself protects β-cells.

Next, we found that a major population of post-BMT islets were located near pancreatic ducts and blood vessels. This observation raises possibilities regarding the origins of post-BMT islets. In general, multipotent adult stem cells are located in somatic tissues, which maintain and regenerate impaired tissues (28, 29). However, there is considerable controversy regarding the existence and location of pancreatic tissue stem cells (30, 31). Previous studies have shown pancreatic stem/progenitor cells in ductal epithelium (24–26). However, recent reports suggest that β-cells arise only from self-duplication of preexisting β-cells, *i.e.* β-cells cannot be derived from non-β-cell progenitors (32, 33). In this study, post-BMT islets were located near pancreatic ducts. In addition, BrdU-positive cells were detected in the vicinity of pancreatic ducts in STZ+BMT mice. After islet numbers had been decreased by STZ, a rise above normoglycemic control levels was seen, indicating new islet formation. In addition, BM-derived cells accumulated in and around post BMT-islets. Thus, BM-derived cells are likely to stimulate proliferation and differentiation of pancreatic stem/progenitor cells in ductal epithelium, resulting in new islet formation. Given the observation that BrdU-positive cells in islets expressed insulin, these cells must still have been proliferative after differentiation into pancreatic β-cells. However, further studies, focusing on the origin of newly generated islets, are needed to support this speculation. Whereas BM-derived cells that accumulated around the islets in STZ+BMT mice were CD45 positive, immunohistochemical studies revealed that these cells do not express mature T or B lymphocyte or macrophage markers. Taken together with the finding that simple BM infusion without preirradiation induced neither β-cell regeneration nor accumulation of BM-derived cells (data not shown), we speculate that these immature BM-derived cells send signals triggering proliferation and differentiation of stem/progenitor cells into β-cells. Our next goal is identification of these signals.

To examine the causal relationship between BM-derived cell mobilization and BMT-induced β-cell regeneration, we performed similar experiments using a model of impaired

E, the *thick line* indicates STZ-treated *Nos3*$^{+/+}$ mice receiving BMT from *Nos3*$^{+/+}$ mice, and the *dotted line* STZ-treated *Nos3*$^{-/-}$ mice receiving BMT from *Nos3*$^{-/-}$ mice. *, $P < 0.05$ between STZ-treated *Nos3*$^{+/+}$ mice receiving BMT from *Nos3*$^{+/+}$ mice and STZ-treated *Nos3*$^{-/-}$ mice receiving BMT from *Nos3*$^{-/-}$mice at the same time points. F, Immunostaining of pancreases with antiinsulin and anti-CD45 antibodies. Pancreases from normoglycemic control mice (*Nos3*$^{+/+}$ mouse in a and *Nos3*$^{-/-}$ mouse in f), hyperglycemic control mice (*Nos3*$^{+/+}$ mouse in b and *Nos3*$^{-/-}$ mouse in g), STZ-treated *Nos3*$^{+/+}$ mice receiving BMT from *Nos3*$^{+/+}$ mice (7 d after BMT in c and d, 14 d after BMT in e), and STZ-treated *Nos3*$^{-/-}$ mice receiving BMT from *Nos3*$^{-/-}$ mice (7 d after BMT in h and i, 14 d after BMT in j). *Green* indicates insulin-positive, *red* CD45-positive cells. *Red arrows* indicate CD45-positive cells in and around islets and *white arrows* pancreatic ducts and blood vessels.

BM-derived cell mobilization. Mechanisms underlying mobilization of hematopoietic and endothelial progenitor cells from BM after myelosuppression have been studied in detail (34). After myelosuppression, secreted cytokines/chemokines, such as granulocyte-colony stimulating factor, stromal cell-derived factor, and vascular endothelial growth factor, activate matrix metalloproteinase (MMP)-9 in the BM microenvironment. Activated MMP-9 processes membrane-bound kit-ligand, releases it as soluble kit-ligand (sKitL), followed by binding of sKitL to c-*kit* on the stem cell surface and stimulation of its mobilization from the BM. Because nitric oxide from BM is necessary for MMP-9 activation, sKitL production and the resultant mobilization of BM-derived cells are impaired in *Nos3*$^{-/-}$ mice (20). Therefore, using *Nos3*$^{-/-}$ mice, we examined the effects of BMT on blood glucose levels and glucose β-cell regeneration. We first confirmed that recovery of the WBC count after BMT was significantly delayed in *Nos3*$^{-/-}$ to *Nos3*$^{-/-}$ mice, compared with *Nos3*$^{+/+}$ to *Nos3*$^{+/+}$ mice. Judging from the doubling time of hematopoietic cells, a 1-wk delay in WBC recovery indicates marked impairment of BM cell mobilization by approximately 2 orders of magnitude. In *Nos3*$^{-/-}$ to *Nos3*$^{-/-}$ mice, BMT had virtually no effects on blood glucose levels, pancreatic insulin contents, islet numbers, or percentage of BrdU-positive cells among islet cells. In addition, far fewer CD45-positive cells were detected in and around islets. These results support the notion that BMT-induced BM-derived cell mobilization plays a pivotal role in β-cell regeneration from ductal progenitor cells.

Neovascularization in ischemic regions is also impaired in *Nos3*$^{-/-}$ mice because of decreased mobilization of BM-derived endothelial progenitor cells (20). The microvasculature is well developed in pancreatic islets (35). Endothelial signals are reportedly important for islet development (36), insulin gene expression, and β-cell proliferation (37). In the present study, a small population of BM-derived cells around regenerated islets was positively stained with CD31, although these cells were largely CD31 negative. This observation is consistent with the results of previous report (14). Therefore, in addition to hematopoietic progenitor cells, endothelial progenitor cells mobilized from BM may contribute to β-cell regeneration after BMT by promoting islet microvasculature formation. In addition, BM-derived endothelial progenitor cells have been shown to contribute to neovascularization in impaired tissues, including myocardial (38) and hind limb ischemia (39). Recruitment of these cells reportedly occurs in response to acute injury of β-cells (19). Taken together with the finding that, when BMT was performed 30 d after STZ treatment, hyperglycemia-improving effects were far smaller, acute STZ injury might trigger migration of immature BM-derived cells to the injured pancreas.

We do not rule out the importance of eNOS in pancreatic blood vessels for BMT-induced β-cell regeneration. However, in *Nos3*$^{-/-}$ to *Nos3*$^{+/+}$ mice, which have decreased BM eNOS (because of BM replacement with eNOS-deficient cells) with intact pancreatic eNOS, the blood glucose-lowering effects of BMT were significantly blunted, compared with *Nos3*$^{+/+}$ to *Nos3*$^{+/+}$ mice. Thus, glucose-lowering effects correlated inversely with the severity of myelosuppression and delayed recovery of the peripheral WBC count, suggesting the importance of BM-derived cell mobilization, rather than eNOS activity in pancreatic blood vessels, in BMT-induced β-cell regeneration.

In summary, BMT promotes β-cell regeneration after STZ-induced injury. A series of BMT experiments using *Nos3*$^{-/-}$ mice demonstrated BM-derived cell mobilization to be essential for BMT-induced β-cell regeneration. Acute injury with STZ treatment may trigger recruitment of immature BM-derived cells to the injured pancreas. Recruited BM-derived cells may then stimulate stem/progenitor cells located in the recipient pancreas, resulting in islet regeneration. To our knowledge, this is the first report showing mobilization of BM-derived cells to be involved in β-cell regeneration in diabetic animals. From the viewpoint of clinical application, it is important to study the effects of myelosuppression-inducing reagents, such as antitumor drugs, on pancreatic islet regeneration.

Acknowledgments

The authors thank Dr. M. Okabe for providing GFP transgenic mice and are indebted to M. Hoshi, I. Sato, K. Kawamura, and J. Fushimi, who assisted with various aspects of this study.

Received October 5, 2006. Accepted January 18, 2007.

Address all correspondence and requests for reprints to: Hideki Katagiri, M.D., Ph.D., Division of Advanced Therapeutics for Metabolic Diseases, Center for Translational and Advanced Animal Research, Tohoku University Graduate School of Medicine, 2-1 Seiryo-machi, Aoba-ku, Sendai 980-8575, Japan. E-mail: katagiri@mail.tains.tohoku.ac.jp.

This work was supported by a Grant-in-Aid for Young Scientists, B (16790503) (to T.O.), a Grant-in-Aid for Scientific Research (B2, 18390267) (to H.K.) from the Ministry of Education, Science, Sports, and Culture of Japan, and a Grant-in-Aid for Scientific Research (H16-genome-003) (to Y.O.) from the Ministry of Health, Labor, and Welfare of Japan. This work was also supported by grants from the 21st Century COE Program "CRESCENDO" (to H.K.) and "the Center for Innovative Therapeutic Development for Common Diseases" (to Y.O.) from the Ministry of Education, Science, Sports, and Culture of Japan.

Disclosure Statement: The authors have nothing to disclose.

References

1. **Krause DS, Theise ND, Collector MI, Henegariu O, Hwang S, Gardner R, Neutzel S, Sharkis SJ** 2001 Multi-organ, multi-lineage engraftment by a single bone marrow-derived stem cell. Cell 105:369–377
2. **Sata M, Saiura A, Kunisato A, Tojo A, Okada S, Tokuhisa T, Hirai H, Makuuchi M, Hirata Y, Nagai R** 2002 Hematopoietic stem cells differentiate into vascular cells that participate in the pathogenesis of atherosclerosis. Nat Med 8:403–409
3. **Takahashi T, Kalka C, Masuda H, Chen D, Silver M, Kearney M, Magner M, Isner JM, Asahara T** 1999 Ischemia- and cytokine-induced mobilization of bone marrow-derived endothelial progenitor cells for neovascularization. Nat Med 5:434–438
4. **Ferrari G, Cusella-De Angelis G, Coletta M, Paolucci E, Stornaiuolo A, Cossu G, Mavilio F** 1998 Muscle regeneration by bone marrow-derived myogenic progenitors. Science 279:1528–1530
5. **Orlic D, Kajstura J, Chimenti S, Jakoniuk I, Anderson SM, Li B, Pickel J, McKay R, Nadal-Ginard B, Bodine DM, Leri A, Anversa P** 2001 Bone marrow cells regenerate infarcted myocardium. Nature 410:701–705
6. **Okamoto R, Yajima T, Yamazaki M, Kanai T, Mukai M, Okamoto S, Ikeda Y, Hibi T, Inazawa J, Watanabe M** 2002 Damaged epithelia regenerated by bone marrow-derived cells in the human gastrointestinal tract. Nat Med 8:1011–1017
7. **Lee VM, Stoffel M** 2003 Bone marrow: an extra-pancreatic hideout for the elusive pancreatic stem cell? J Clin Invest 111:799–801
8. **Lechner A, Habener JF** 2003 Bone marrow stem cells find a path to the pancreas. Nat Biotechnol 21:755–756
9. **Tessem JS, DeGregori J** 2004 Roles for bone-marrow-derived cells in β-cell maintenance. Trends Mol Med 10:558–564
10. **Ianus A, Holz GG, Theise ND, Hussain MA** 2003 *In vivo* derivation of

glucose-competent pancreatic endocrine cells from bone marrow without evidence of cell fusion. J Clin Invest 111:843–850
11. **Choi JB, Uchino H, Azuma K, Iwashita N, Tanaka Y, Mochizuki H, Migita M, Shimada T, Kawamori R, Watada H** 2003 Little evidence of transdifferentiation of bone marrow-derived cells into pancreatic β cells. Diabetologia 46:1366–1374
12. **Lechner A, Yang YG, Blacken RA, Wang L, Nolan AL, Habener JF** 2004 No evidence for significant transdifferentiation of bone marrow into pancreatic β-cells *in vivo*. Diabetes 53:616–623
13. **Taneera J, Rosengren A, Renstrom E, Nygren JM, Serup P, Rorsman P, Jacobsen SE** 2006 Failure of transplanted bone marrow cells to adopt a pancreatic β-cell fate. Diabetes 55:290–296
14. **Hess D, Li L, Martin M, Sakano S, Hill D, Strutt B, Thyssen S, Gray DA, Bhatia M** 2003 Bone marrow-derived stem cells initiate pancreatic regeneration. Nat Biotechnol 21:763–770
15. **Banerjee M, Kumar A, Bhonde RR** 2005 Reversal of experimental diabetes by multiple bone marrow transplantation. Biochem Biophys Res Commun 328: 318–325
16. **Izumida Y, Aoki T, Yasuda D, Koizumi T, Suganuma C, Saito K, Murai N, Shimizu Y, Hayashi K, Odaira M, Kusano T, Kushima M, Kusano M** 2005 Hepatocyte growth factor is constitutively produced by donor-derived bone marrow cells and promotes regeneration of pancreatic β-cells. Biochem Biophys Res Commun 333:273–282
17. **Li FX, Zhu JW, Tessem JS, Beilke J, Varella-Garcia M, Jensen J, Hogan CJ, DeGregori J** 2003 The development of diabetes in E2f1/E2f2 mutant mice reveals important roles for bone marrow-derived cells in preventing islet cell loss. Proc Natl Acad Sci USA 100:12935–12940
18. **Than S, Ishida H, Inaba M, Fukuba Y, Seino Y, Adachi M, Imura H, Ikehara S** 1992 Bone marrow transplantation as a strategy for treatment of non-insulin-dependent diabetes mellitus in KK-Ay mice. J Exp Med 176:1233–1238
19. **Mathews V, Hanson PT, Ford E, Fujita J, Polonsky KS, Graubert TA** 2004 Recruitment of bone marrow-derived endothelial cells to sites of pancreatic β-cell injury. Diabetes 53:91–98
20. **Aicher A, Heeschen C, Mildner-Rihm C, Urbich C, Ihling C, Technau-Ihling K, Zeiher AM, Dimmeler S** 2003 Essential role of endothelial nitric oxide synthase for mobilization of stem and progenitor cells. Nat Med 9:1370–1376
21. **Okabe M, Ikawa M, Kominami K, Nakanishi T, Nishimune Y** 1997 'Green mice' as a source of ubiquitous green cells. FEBS Lett 407:313–319
22. **Wang Z, Dohle C, Friemann J, Green BS, Gleichmann H** 1993 Prevention of high- and low-dose STZ-induced diabetes with D-glucose and 5-thio-D-glucose. Diabetes 42:420–428
23. **Ishihara H, Takeda S, Tamura A, Takahashi R, Yamaguchi S, Takei D, Yamada T, Inoue H, Soga H, Katagiri H, Tanizawa Y, Oka Y** 2004 Disruption of the WFS1 gene in mice causes progressive β-cell loss and impaired stimulus-secretion coupling in insulin secretion. Hum Mol Genet 13:1159–1170
24. **Ramiya VK, Maraist M, Arfors KE, Schatz DA, Peck AB, Cornelius JG** 2000 Reversal of insulin-dependent diabetes using islets generated *in vitro* from pancreatic stem cells. Nat Med 6:278–282
25. **Bonner-Weir S, Taneja M, Weir GC, Tatarkiewicz K, Song KH, Sharma A, O'Neil JJ** 2000 *In vitro* cultivation of human islets from expanded ductal tissue. Proc Natl Acad Sci USA 97:7999–8004
26. **Gao R, Ustinov J, Pulkkinen MA, Lundin K, Korsgren O, Otonkoski T** 2003 Characterization of endocrine progenitor cells and critical factors for their differentiation in human adult pancreatic cell culture. Diabetes 52:2007–2015
27. **Ema H, Suda T, Nakauchi H, Nakamura Y, Iwama A, Imagawa S, Akutsu M, Kano Y, Kato S, Yabe M, Yoshida M, Sakamoto S, Amemiya Y, Miura Y** 1991 Multipotent and committed CD34+ cells in bone marrow transplantation. Jpn J Cancer Res 82:547–552
28. **Tropepe V, Coles BL, Chiasson BJ, Horsford DJ, Elia AJ, McInnes RR, van der Kooy D** 2000 Retinal stem cells in the adult mammalian eye. Science 287:2032–2036
29. **Okano H** 2002 Neural stem cells: progression of basic research and perspective for clinical application. Keio J Med 51:115–128
30. **Trucco M** 2005 Regeneration of the pancreatic β cell. J Clin Invest 115:5–12
31. **Blyszczuk P, Wobus AM** 2004 Stem cells and pancreatic differentiation *in vitro*. J Biotechnol 113:3–13
32. **Dor Y, Brown J, Martinez OI, Melton DA** 2004 Adult pancreatic β-cells are formed by self-duplication rather than stem-cell differentiation. Nature 429: 41–46
33. **Georgia S, Bhushan A** 2004 β Cell replication is the primary mechanism for maintaining postnatal β cell mass. J Clin Invest 114:963–968
34. **Heissig B, Hattori K, Dias S, Friedrich M, Ferris B, Hackett NR, Crystal RG, Besmer P, Lyden D, Moore MA, Werb Z, Rafii S** 2002 Recruitment of stem and progenitor cells from the bone marrow niche requires MMP-9 mediated release of kit-ligand. Cell 109:625–637
35. **Menger MD, Vajkoczy P, Leiderer R, Jager S, Messmer K** 1992 Influence of experimental hyperglycemia on microvascular blood perfusion of pancreatic islet isografts. J Clin Invest 90:1361–1369
36. **Lammert E, Cleaver O, Melton D** 2001 Induction of pancreatic differentiation by signals from blood vessels. Science 294:564–567
37. **Nikolova G, Jabs N, Konstantinova I, Domogatskaya A, Tryggvason K, Sorokin L, Fassler R, Gu G, Gerber HP, Ferrara N, Melton DA, Lammert E** 2006 The vascular basement membrane: a niche for insulin gene expression and β cell proliferation. Dev Cell 10:397–405
38. **Otani A, Kinder K, Ewalt K, Otero FJ, Schimmel P, Friedlander M** 2002 Bone marrow-derived stem cells target retinal astrocytes and can promote or inhibit retinal angiogenesis. Nat Med 8:1004–1010
39. **Higashi Y, Kimura M, Hara K, Noma K, Jitsuiki D, Nakagawa K, Oshima T, Chayama K, Sueda T, Goto C, Matsubara H, Murohara T, Yoshizumi M** 2004 Autologous bone-marrow mononuclear cell implantation improves endothelium-dependent vasodilation in patients with limb ischemia. Circulation 109:1215–1218

Endocrinology **is published monthly by The Endocrine Society (http://www.endo-society.org), the foremost professional society serving the endocrine community.**

Am J Physiol Cell Physiol 293: C1576–C1585, 2007.
First published July 5, 2007; doi:10.1152/ajpcell.00570.2006.

Carboxy-terminal modulator protein induces Akt phosphorylation and activation, thereby enhancing antiapoptotic, glycogen synthetic, and glucose uptake pathways

Hiraku Ono,[1]* Hideyuki Sakoda,[2]* Midori Fujishiro,[2] Motonobu Anai,[1] Akifumi Kushiyama,[2] Yasushi Fukushima,[2] Hideki Katagiri,[3] Takehide Ogihara,[3] Yoshitomo Oka,[3] Hideaki Kamata,[5] Nanao Horike,[4] Yasunobu Uchijima,[4] Hiroki Kurihara,[4] and Tomoichiro Asano[5]

[1]*Department of Endocrinology and Metabolism, Institute for Adult Disease, Asahi Life Foundation, Chiyoda-ku, Tokyo;* [2]*Department of Internal Medicine, Graduate School of Medicine, University of Tokyo, Bunkyo-ku, Tokyo;* [3]*Division of Advanced Therapeutics for Metabolic Diseases, Department of Translational Research, Tohoku University, Graduate School of Medicine, Aoba-ku, Sendai, Miyagi;* [4]*Department of Physiological Chemistry and Metabolism, Graduate School of Medicine, University of Tokyo, Bunkyo-ku, Tokyo; and* [5]*Department of Medical Science, Graduate School of Medicine, University of Hiroshima, Minami-ku, Hiroshima City, Hiroshima, Japan*

Submitted 9 November 2006; accepted in final form 3 July 2007

Ono H, Sakoda H, Fujishiro M, Anai M, Kushiyama A, Fukushima Y, Katagiri H, Ogihara T, Oka Y, Kamata H, Horike N, Uchijima Y, Kurihara H, Asano T. Carboxy-terminal modulator protein induces Akt phosphorylation and activation, thereby enhancing antiapoptotic, glycogen synthetic, and glucose uptake pathways. *Am J Physiol Cell Physiol* 293: C1576–C1585, 2007. First published July 5, 2007; doi:10.1152/ajpcell.00570.2006.—Carboxy-terminal modulator protein (CTMP) was identified as binding to the carboxy terminus of Akt and inhibiting the phosphorylation and activation of Akt. In contrast to a previous study, we found CTMP overexpression to significantly enhance Akt phosphorylation at both Thr^{308} and Ser^{473} as well as the kinase activity of Akt, while phosphatidylinositol 3-kinase (PI3-kinase) activity was unaffected. Translocation of Akt to the membrane fraction was also markedly increased in response to overexpression of CTMP, with no change in the whole cellular content of Akt. Furthermore, the phosphorylations of GSK-3β and Foxo1, well-known substrates of Akt, were increased by CTMP overexpression. On the other hand, suppression of CTMP with small interfering RNA partially but significantly attenuated this Akt phosphorylation. The cellular activities reportedly mediated by Akt activation were also enhanced by CTMP overexpression. UV-B-induced apoptosis of HeLa cells was significantly reversed not only by overexpression of the active mutant of Akt (myr-Akt) but also by that of CTMP. Increases in glucose transport activity and glycogen synthesis were also induced by overexpression of either myr-Akt or CTMP in 3T3-L1 adipocytes. Taking these results into consideration, it can be concluded that CTMP induces translocation of Akt to the membrane and thereby increases the level of Akt phosphorylation. As a result, CTMP enhances various cellular activities that are principally mediated by the PI3-kinase/Akt pathway.

phosphatidylinositol 3-kinase

SERINE/THREONINE KINASE Akt has been established as one of the most important molecules in intracellular signaling cascades of growth hormones including insulin (9, 13, 22, 26, 44, 51). Its activation mechanisms have been clarified to some extent in recent years (1, 7): tyrosine kinase-type growth hormone receptors activate phosphatidylinositol 3-kinase (PI3-kinase), which generates 3-phosphoinositides on the plasma membrane. Akt is then recruited to the membrane through the binding of its PH domain and these 3-phosphoinositides (6, 19). When Akt reaches the membrane, two phosphorylation sites (Thr^{308} and Ser^{473}) of Akt are phosphorylated by phosphoinositide-dependent kinase (PDK)-1 (45, 46) and by PDK-2 (18, 28, 38, 39, 50), respectively. Recent reports have indicated that PDK-2 is very likely to be the mammalian target of rapamycin (mTOR)-Rictor complex (24, 43). Once phosphorylated at both sites, Akt is fully activated.

Recently, several proteins that modify the Akt activation state via direct binding to Akt (2, 4, 14, 34, 40) have been identified. Among them, carboxy-terminal modulator protein (CTMP) (23, 34) was reported to bind to the carboxy-terminal regulatory domain of Akt and to inhibit its activation. In addition, it was shown that stable CTMP overexpression in AKT8 cells inhibits tumor growth in nude mice. However, Akt is related not only to cell proliferation but also to antiapoptosis (12, 29, 35) and glucose metabolic processes such as glycogen synthesis, gluconeogenesis, glycolysis, and glucose uptake (16, 21, 25, 32, 47, 48, 51). The effects of CTMP on insulin signaling and on glucose metabolism have not previously been examined. Therefore, the initial aim of this study was to determine whether CTMP is a molecule involved in the insulin sensitivity of glucose metabolic processes, via its effect on Akt activity.

However, in our study, overexpression of CTMP was demonstrated to obviously enhance Akt phosphorylation regardless of whether a transient or a stable expression system was used. To our surprise, this is quite the opposite of previously reported results. When endogenous CTMP was suppressed by small interfering RNA (siRNA), Akt phosphorylations were reduced. Moreover, several cellular functions downstream from Akt, such as antiapoptotic and glucose metabolic processes, were shown to be enhanced by CTMP. We thus conclude that CTMP is a positive regulator of Akt.

* H. Ono and H. Sakoda contributed equally to this work.

Address for reprint requests and other correspondence: T. Asano, Dept. of Medical Science, Graduate School of Medicine, Univ. of Hiroshima, 1-2-3 Kasumi, Minami-ku, Hiroshima City, Hiroshima 734-8551, Japan (e-mail: tasano@hiroshima-u.ac.jp).

The costs of publication of this article were defrayed in part by the payment of page charges. The article must therefore be hereby marked "*advertisement*" in accordance with 18 U.S.C. Section 1734 solely to indicate this fact.

MATERIALS AND METHODS

Antibodies and immunoblotting. Anti-CTMP antibody was raised by immunizing rabbits with the keyhole limpet hemocyanin-conjugated 17 carboxy-terminal amino acids of CTMP and affinity purified on Affi-Gel-10 (Bio-Rad, Hercules, CA) columns to which the corresponding peptide had been coupled. The animal protocol was approved by the University of Tokyo Ethics Committee for Animal Experiments and strictly adhered to the guidelines for animal experiments of the University of Tokyo. Anti-Akt antibody was described previously (37). Anti-phospho-Thr^{308} Akt, anti-phospho-Ser^{473} Akt, anti-phospho-Ser^{9} GSK-3β, and anti-phospho-Ser^{256} Foxo1 were purchased from Cell Signaling Technology (Beverly, MA). Anti-phosphotyrosine antibody (4G10) was purchased from Upstate Biotechnology (Lake Placid, NY). Immunoblotting was carried out with enhanced chemiluminescence (ECL Detection Kit, Amersham), and representative blots were obtained by exposing the films. The bands were quantitatively analyzed with Molecular Imager FX (Bio-Rad) without exposure of the films.

DNA constructs, expression vectors, and adenoviruses. Complete cDNA of human CTMP was amplified by PCR from a cDNA library of HeLa cells with a primer set based on the reported sequence (34). Amino-terminal FLAG tag was added, also by PCR. All the sequences were confirmed with a CEQ-2000XL DNA sequencer (Beckman Coulter, Tokyo, Japan). To prepare the plasmid expression vector, cDNA was subcloned into pcDNA3.1(−) (Invitrogen, Carlsbad, CA). To prepare the adenovirus for CTMP expression, the DNA construct was subcloned into a pAdexCAwt cosmid cassette and transfected with the parental viral genome into HEK293 cells as described previously (27). Adenovirus vectors for carboxy-terminally myc-tagged wild-type (WT) Akt, carboxy-terminally myc-tagged myr-Akt, and *Escherichia coli* β-galactosidase (LacZ) were described previously (27, 52). Adenoviruses were concentrated and purified by ultracentrifugation in a CsCl gradient as described previously (33).

Cell culture, adenoviral infection, and serum starvation. COS-1, HepG2, HeLa, and NIH3T3 cells were cultured in DMEM containing 4.5 g/l glucose, penicillin-streptomycin (Pen/Strep), and 10% fetal

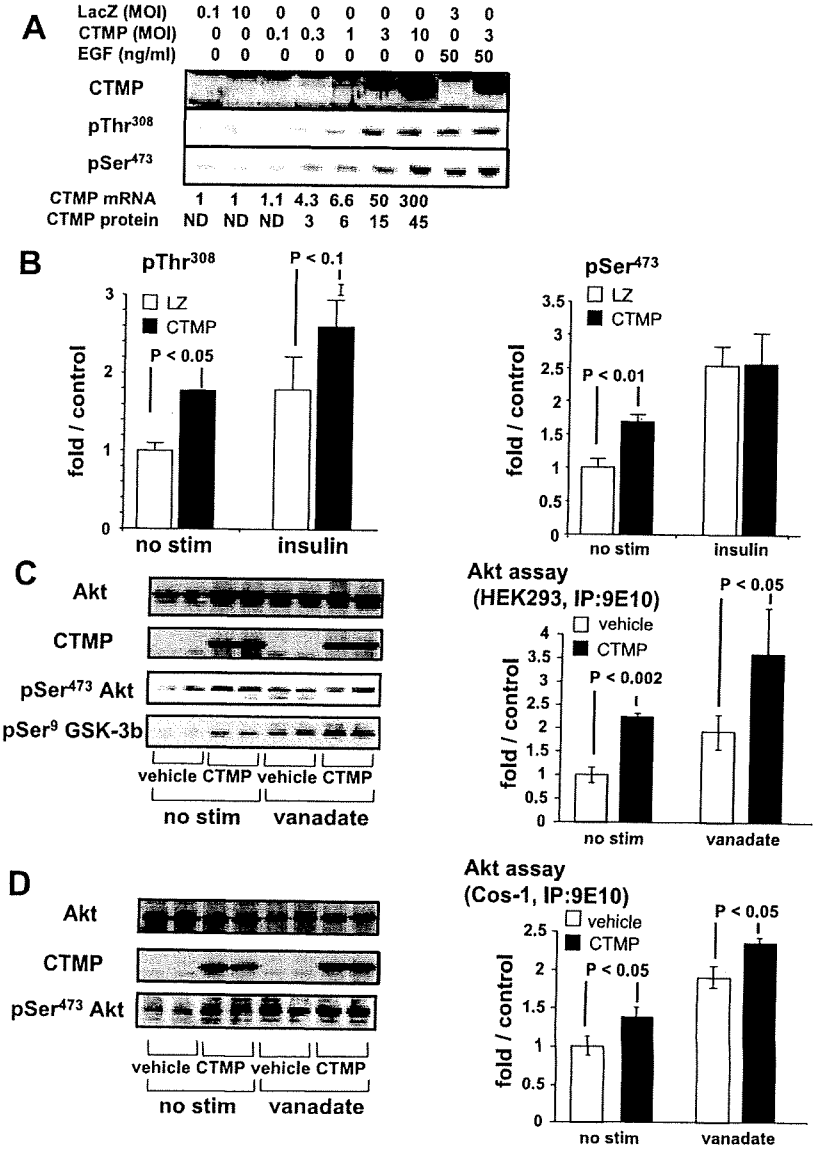

Fig. 1. Effects of transiently overexpressed carboxy-terminal modulator protein (CTMP) on Akt phosphorylation and activation. *A*: COS-1 cells were infected with various titers [multiplicity of infection (MOI) = 0.1–10] of LacZ or CTMP adenovirus. Phosphorylations of endogenous Akt at Thr^{308} or Ser^{473} without or with 50 ng/ml EGF stimulation were assayed by Western blotting with phospho-specific antibodies. Representative bands from duplicate experiments are shown. The multiplicity of CTMP expression at its mRNA level or protein level was assayed, and is shown at *bottom*. The protein level is indicated by inequality, because our antibody could not detect endogenous CTMP [not detected (ND)]. LacZ did not influence Akt phosphorylations, regardless of its MOI or EGF stimulation. CTMP enhanced these phosphorylations in a dose-dependent manner in the nonstimulated (basal) state. CTMP did not suppress Akt phosphorylations even when the cells were stimulated with EGF. *B*: HepG2 cells were infected with CTMP or LacZ (LZ) with adenoviral vectors. Phosphorylations of endogenous Akt at Thr^{308} (*left*) or Ser^{473} (*right*) in HepG2 cells without (no stim) or with 100 nM insulin stimulation were assayed as in *A* and quantified in experiments performed in triplicate. Values are mean ± SE fold increase over LacZ without insulin. The enhancing effect of CTMP on Akt phosphorylation was also observed in HepG2 cells. *C*: Akt phosphorylation and kinase activity were assayed in HEK293 cells. HEK293 cells were transfected with the expression vector containing CTMP cDNA and were coexpressed with wild-type Akt with adenoviral vectors. *Left*: overexpression of CTMP and CTMP-induced increases in phosphorylations of Akt and GSK-3β. *Right*: CTMP-induced increase in Akt kinase activity with or without vanadate stimulation. Values are mean ± SE fold increase over vehicle without stimulation. ANOVA confirmed the significance of the enhancing effect of CTMP on Akt activity. *D*: Akt phosphorylation and kinase activity were assayed in COS-1 cells transfected with the expression vector containing CTMP cDNA. *Right*: overexpression of CTMP and CTMP-induced increases in phosphorylations of Akt. *Left*: CTMP-induced increase in Akt kinase activity with or without vanadate stimulation. Values are mean ± SE fold increase over vehicle without stimulation. ANOVA confirmed the significance of the enhancing effect of CTMP on Akt activity. CTMP or vehicle was coexpressed with wild-type Akt with adenoviral vectors. The effect of CTMP on Akt phosphorylations was enhanced. IP, immunoprecipitation.

calf serum (FCS) under a 5% CO_2 atmosphere at 37°C. Adenoviral infection and serum starvation were carried out simultaneously for these cell types 24 h before the following experiments, i.e., the cells were incubated with adenovirus for 1 h, washed once with serum-free DMEM containing 0.2% BSA, and then incubated with that serum-free medium for 24 h. NIH3T3 cells stably transfected with CTMP constructs (pcDNA) were selected and maintained in DMEM containing 500 mg/l Geneticin. 3T3-L1 adipocytes were prepared from 3T3-L1 fibroblasts as described previously (41). Four days after the induction of differentiation, at which time >90% of the 3T3-L1 cells expressed the adipocyte phenotype, viral infection of these cells was carried out. Serum starvation of 3T3-L1 adipocytes is described below.

Plasmid transfection and Akt kinase assay. COS-1 cells or HEK293 cells were maintained in DMEM supplemented with 10% FCS (Life Technologies) and 50 U/ml Pen/Strep (GIBCO). Transfections were performed with the calcium phosphate technique (34). To obtain a cell line stably overexpressing CTMP, selection was carried out with G-418 after plasmid transfection.

After cells were first serum starved for 12 h in serum-free DMEM, they were stimulated with 100 μM pervanadate for 10 min at 37°C. Next, the cells were lysed in lysis buffer [mM: 50 Tris·HCl (pH 7.5), 150 NaCl, 1 EDTA, 1 EGTA, 2.5 sodium pyrophosphate, 1 sodium orthovanadate, 1 β-glycerophosphate, and 0.2 PMSF, with 1% Triton X-100] and centrifuged. The supernatants were then immunoprecipitated with anti-myc antibodies and protein G Sepharose beads. The immunoprecipitants were washed three times with lysis buffer and twice with kinase assay buffer [mM: 50 Tris·HCl (pH 7.5), 10 $MgCl_2$, 1 EGTA, and 1 dithiothreitol]. Beads were resuspended in 45 μl of kinase assay buffer, and reactions were initiated by the addition of 5 μl of an ATP mixture containing 5 μM nonradioactive ATP, 2 μCi of [γ-^{32}P]ATP (4,000 Ci/mmol), and 5 μM Crosstide and then incubated for 30 min at 30°C. The kinase reaction mixture was spotted onto a P81 filter (Whatman), the filters were washed three times with 0.5% (wt/vol) orthophosphoric acid, and the radioactivity remaining on the filters was measured with a BAStation2000 (Fujifilm).

Adenoviral gene transfer and Akt kinase assay. COS-1 cells in 10-cm dishes, 24 h after serum starvation and viral infection [multiplicity of infection (MOI) 3], were stimulated without or with 50 ng/ml EGF for 10 min, washed once with ice-cold PBS, and lysed with 1 ml/dish of lysis buffer from an Akt kinase assay kit (Cell Signaling Technology). Insoluble materials were eliminated by centrifugation, and 200 μl of the supernatants was immunoprecipitated with 10 μl of immobilized Akt monoclonal antibody. Subsequent steps were carried out according to the manufacturer's instructions.

RNA silencing of CTMP in HeLa cells. HeLa cells were seeded at 1×10^4 cells/well onto 24-well plates. At 24 h after seeding, siRNAs were transfected, i.e., 0.25 μg of siRNA of CTMP (target sequence: AAGCATGAAGAATAAATACAT) or lamin (control siRNA, target sequence: AACTGGACTTCCAGAAGAACA), 1.5 μl of RNAiFect transfection reagent (Qiagen, Tokyo, Japan), and DMEM containing 10% FCS (total 100 μl/well) were mixed, incubated for 10 min, and dropped into each well. At 36 h after transfection, cells were serum starved. After 12 h of starvation, the cells were stimulated without or with 1 μM insulin for 15 min and lysed with the lysis buffer from an RNAqueous kit (Ambion, Austin, TX) or Laemmli buffer.

Total RNA was purified with the RNAqueous kit according to the manufacturer's instructions. RNA was then reverse transcribed with Superscript III (Invitrogen). cDNA levels of CTMP and GAPDH (internal standard) were quantified with LightCycler and DNA Master SYBR Green I (Roche Diagnostics, Tokyo, Japan). The primer sequences used were TCTGAGGAAGTCATTCTTAAG and CTCATCAACACTCTGAACATT for CTMP and GAAGGTGAAGGTCGGAGTC and GAAGATGGTGATGGGATTTC for GAPDH.

Subcellular fractionation. In a 15-cm dish, COS-1 cells (24 h after virus infection at MOI 3) were washed with PBS and scraped off into 2 ml of HES (mM: 20 HEPES pH 7.4, 1 EDTA, 250 sucrose) containing protease/phosphatase inhibitors (mM: 1 PMSF, 1 orthovanadate, 40 β-glycerophosphate, 50 NaF). The cell suspension was homogenized with 10 strokes of a Teflon homogenizer and centrifuged at 600 *g* for 15 min to eliminate the nuclear fraction. The supernatant was ultracentrifuged at 250,000 *g* for 90 min, and the pellet was rinsed once with HES and lysed with 100 μl of lysis buffer (mM: 50 Tris pH 7.4, 100 NaCl, 10 EDTA, with 10% glycerol and 1% Nonidet P-40) containing protease/phosphatase inhibitors. The lysate was then recentrifuged at 15,000 *g* for 15 min to eliminate the cytoskeletal fraction. The supernatant was taken as the membrane fraction.

PI3-kinase activity assay. COS-1 cells in 12-well culture plates, 24 h after serum starvation and viral infection (MOI 3), were stimulated

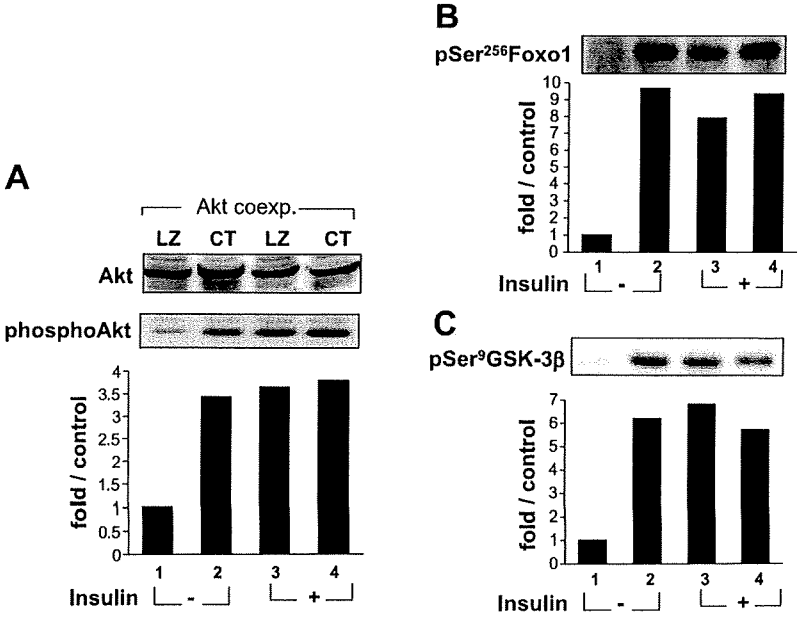

Fig. 2. Positive effect of CTMP on Foxo1 and GSK-3β phosphorylations in HeLa cells. HeLa cells were infected with adenovirus to overexpress LacZ (LZ) or CTMP (CT) with wild-type Akt and stimulated without or with 100 nM insulin for 15 min. *A*: overexpressed Akt was confirmed with Western blotting using anti-myc antibody (*top*). Phosphorylation of overexpressed Akt at Thr^{308} was assayed by Western blotting (*middle*), and phosphorylation levels were quantified (*bottom*). *B* and *C*: phosphorylation of Ser^{256} of Foxo1 and Ser^{9} of GSK-3β were assayed by Western blotting with the respective phospho-specific antibodies (*B* and *C*, *top*, respectively), and phosphorylation levels were quantified (*B* and *C*, *bottom*, respectively).

without or with 50 ng/ml EGF or 100 nM sodium orthovanadate for 10 min, washed once with ice-cold PBS, and lysed with lysis buffer (PBS containing 1% Nonidet P-40, 0.35 mg/ml PMSF, and 100 mM sodium orthovanadate). Insoluble materials were eliminated by centrifugation, and the supernatants were immunoprecipitated with anti-phosphotyrosine antibodies and protein G Sepharose. The PI3-kinase activity in the immunoprecipitants was measured as described previously (27).

UV-B irradiation and MTT assay of HeLa cells. HeLa cells were plated onto a 96-well culture plate at a density of 1×10^4 cells/well. At 24 h after seeding, the cells were infected with adenoviruses at an MOI of 3 for 1 h. After infection, the cells were washed once with serum-free DMEM containing 0.2% BSA and incubated in the same medium for 12 h. The medium was then replaced with PBS, and the plate was irradiated with UV-B (wavelength = 312 nm, energy = 8 mW/cm^2; DT-20MCP UV illuminator, ATTO, Tokyo, Japan) for 6 min from the bottom face of the plate. The PBS was then replaced with 100 μl of serum-free DMEM containing 0.2% BSA, and the cells were incubated at 37°C. At 8 h after the irradiation, 10 μl of 12 mM 4,5-dimethylthiazol-2-yl-2,5-diphenyltetrazolium bromide (MTT) solution in PBS was added to each well, and the 37°C incubation was continued for 4 h. One hundred microliters of 10 mM HCl containing 10% SDS was added to each well. After vigorous mixing of each well by pipetting, the plate was incubated at 37°C for 2 h, each well was pipetted again, and absorbance at 570 nm was measured with a microplate reader. Each treatment combination (virus and UV irradiation) was examined four times ($n = 4$).

2-Deoxyglucose uptake assay. 3T3-L1 adipocytes in 24-well culture plates were infected with adenovirus at an MOI of 100. At 45 h after infection, the cells were washed once with DMEM containing 0.2% BSA and incubated in that medium for 3 h for serum starvation.

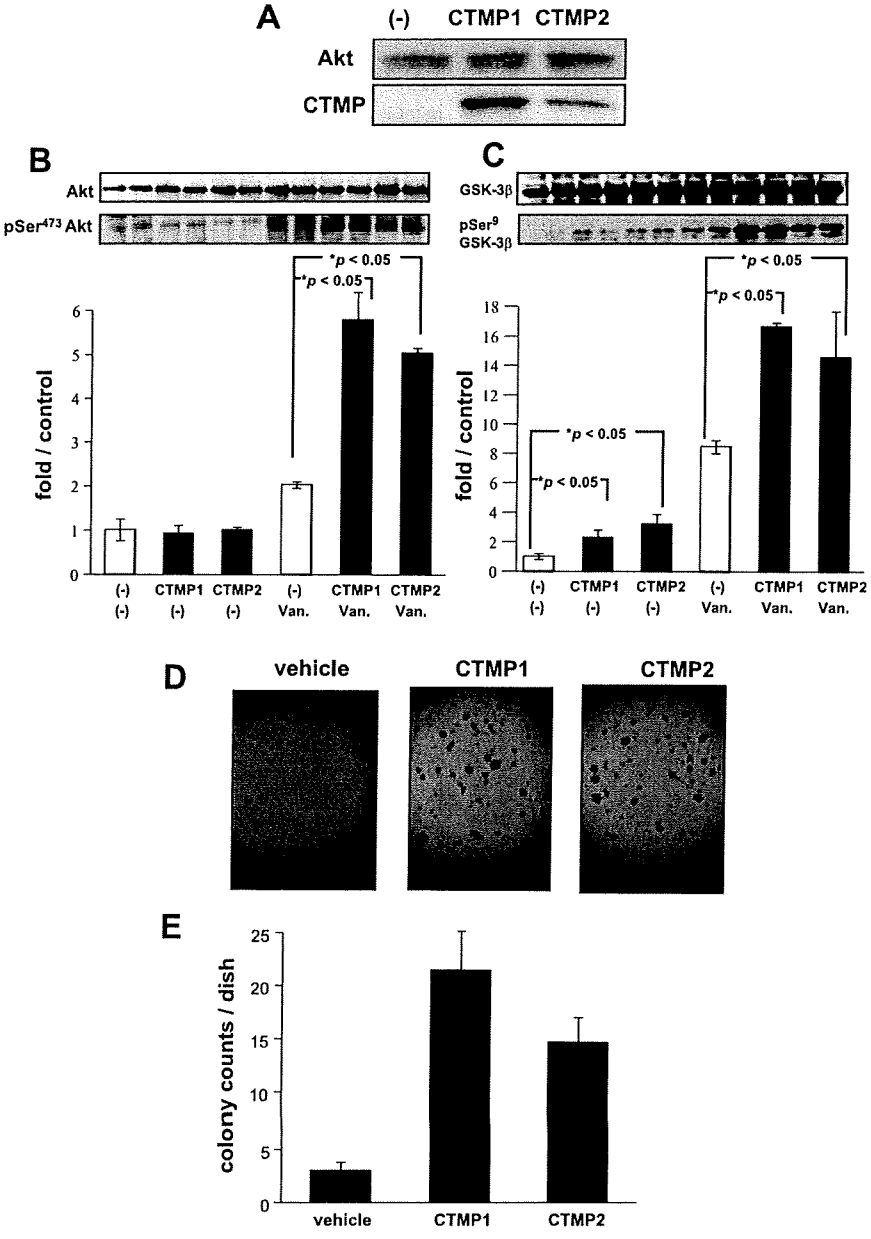

Fig. 3. Effects of stably overexpressed CTMP on Akt and GSK-3β phosphorylations in NIH3T3 cells. NIH3T3 cells were transfected with the expression vector containing CTMP cDNA and subjected to G-418 selection. Control cells were transfected with the expression vector alone, i.e., without CTMP cDNA. *A*: 2 representative cell lines (CTMP1 and CTMP2) overexpressing CTMP were isolated (*bottom*), and the absence of significant alteration of Akt expression was confirmed (*top*). *B* and *C*: Akt (*B*) and GSK-3β (*C*) phosphorylations were examined in the control and 2 CTMP overexpressing cell lines in the absence or presence of vanadate stimulation (Van). *D* and *E*: soft agar assays demonstrating transformation of NIH3T3 fibroblasts by CTMP. For the soft agar assay, NIH3T3 cells stably transfected with CTMP constructs were trypsinized, suspended in DMEM containing 0.3% agar and 20% fetal calf serum, and plated onto a bottom layer containing 0.6% agar. Cells were plated at a density of 2×10^4 cells per 3.5-cm dish. Colonies >0.5 mm in diameter were counted after 14 days (*E*). Four independent experiments were performed, and similar results were obtained.